

Recovering the original simplicity: succinct and deterministic quantum algorithm for the welded tree problem

Guanzhong Li

Sun Yat-sen University

Lvzhou Li

`lilvzh@mail.sysu.edu.cn`

Sun Yat-sen University

Jingquan Luo

Sun Yat-sen University

Research Article

Keywords: the welded tree problem, quantum walk, quantum algorithm

Posted Date: January 12th, 2024

DOI: <https://doi.org/10.21203/rs.3.rs-3842897/v1>

License:   This work is licensed under a Creative Commons Attribution 4.0 International License.

[Read Full License](#)

Additional Declarations: No competing interests reported.

Version of Record: A version of this preprint was published at Algorithmica on October 4th, 2024. See the published version at <https://doi.org/10.1007/s00453-024-01273-w>.

Recovering the original simplicity: succinct and deterministic quantum algorithm for the welded tree problem *

Guanzhong Li[†], Lvzhou Li[†], Jingquan Luo[†]

Institute of Quantum Computing and Software, School of Computer Science and Engineering, Sun Yat-sen University, Guangzhou, 510006, China.

*Corresponding author(s). E-mail(s): lilvzh@mail.sysu.edu.cn;

Contributing authors: ligzh9@mail2.sysu.edu.cn;

luojq25@mail2.sysu.edu.cn;

[†]These authors contributed equally to this work.

Abstract

This work revisits quantum algorithms for the well-known welded tree problem, proposing a very succinct quantum algorithm based on the simplest coined quantum walks. It simply iterates the naturally defined coined quantum walk operator for a predetermined time and finally measure, where the predetermined time can be efficiently computed on classical computers. Then, the algorithm returns the correct answer deterministically, and achieves exponential speedups over any classical algorithm. The significance of the results may be seen as follows. (i) Our algorithm is rather simple compared with the one in (Jeffery and Zur, STOC'2023), which not only breaks the stereotype that coined quantum walks can only achieve quadratic speedups over classical algorithms, but also demonstrates the power of the simplest quantum walk model. (ii) Our algorithm theoretically achieves certainty of success, which is not possible with existing methods. Thus, it becomes one of the few examples that exhibit exponential separation between deterministic (exact) quantum and randomized query complexities, which may also change people's perception that since quantum mechanics is inherently probabilistic, it is impossible to have a deterministic quantum algorithm with exponential speedups for the welded tree problem.

Keywords: the welded tree problem, quantum walk, quantum algorithm

*This work was originally presented at SODA2024 conference.

1 Introduction

A primary goal of the field of quantum computing is to design quantum algorithms that can solve problems faster than classical algorithms. Quantum walks have developed into a fundamental tool for algorithmic design. Since Aharonov et al. [1] first coined the term “quantum walks” thirty years ago, quantum walks have become a major research subject both in theory and in experiment [2–5]. There are two kinds of quantum walks: discrete time quantum walks (DTQW) and continuous time quantum walks (CTQW). Whereas CTQW evolve a Hamiltonian H (related to the graph under consideration) for any time t , i.e. simulating e^{iHt} , DTQW can only evolve the system for discrete time steps, i.e. applying U_{walk}^h to the initial state for some integer h and unitary operator U_{walk} .

DTQW can be further divided into many different frameworks. The earliest and simplest is the coined quantum walks [6, 7] consisting of a coin operator C (usually the Grover diffusion) and a shift operator S (usually the flip-flop shift, i.e. SWAP operator). Later, Szegedy proposed a quantum walk framework [8] from the perspective of Markov chains. In this direction, a series of variant frameworks for spatial search have been developed: the MNRS framework [9], the interpolated walk [10], the electric network framework [11] and its finding version [12]. Quantum algorithms based on these frameworks have provided only at most a quadratic speedup when comparing to the best classical algorithm. Typical examples include quantum algorithms for the element distinctness problem [13], matrix product verification [14], triangle finding [15], group commutativity [16], and so on.

In sharp contrast, exponential algorithmic speedups can be obtained based on CTQW for the welded tree problem [17], which makes the welded tree problem of great interest, as it is one of the few problems for which quantum walk-based algorithms are exponentially faster than classical algorithms. Note that earlier studies have shown that quantum walks can solve problems exponentially faster than classical walks [18, 19], but there exist classical efficient algorithms which are not based on a random walk for those problems [17].

Recently, Jeffery and Zur [20] proposed a new DTQW framework—multidimensional quantum walks (an extension of the electric network framework), and then presented a quantum algorithm based on it to solve the welded tree problem, which achieves exponential speedups over classical algorithms. The pursuit of exponential algorithmic speedups based on DTQW is one of the reasons for proposing the framework of multidimensional quantum walks. Actually, Jeffery and Zur [20] claimed that the major drawback of the existing DTQW frameworks is that they can achieve at most a quadratic speedup over the best classical algorithm, but this drawback does not hold for the multidimensional quantum walk framework¹.

In this work, we revisit quantum algorithms for the welded tree problem, proposing a quite succinct quantum algorithm based purely on the simplest coined quantum

¹Ref. [20] claimed “While quantum walk frameworks make it extremely easy to design quantum algorithms, even without an in-depth knowledge of quantum computing, as evidenced by their wide application across domains, the major drawback is that they can achieve at most a quadratic speedup over the best classical algorithm. This is because a quantum walk search algorithm essentially takes a classical random walk algorithm, and produces a quantum algorithm that is up to quadratically better. This drawback does not hold for the multidimensional quantum walk framework”.

walks, which not only maintains the exponential speedup, but also achieves certainty of success theoretically. Thus, our work demonstrates the power of the simplest quantum walk model, and verifies that a good quantum algorithm does not necessarily resort to complex techniques.

1.1 Coined Quantum Walk

For a graph $G = (V, E)$ and $u \in V$, $\text{deg}(u) = \{v : (u, v) \in E\}$ denotes the set of neighbours of u , and the degree of u is denoted as $d_u = |\text{deg}(u)|$. A coined quantum walk on $G = (V, E)$ is defined on the state space $\mathbb{H}^{N^2} = \text{span}\{|uv\rangle, u, v \in V\}$ with $N = |V|$. The evolution operator of the coined quantum walk at each step is $U_{\text{walk}} = SC$. C , the coin operator, is defined by $C = \sum_{u \in V} |u\rangle\langle u| \otimes C_u$, where C_u is typically the Grover diffusion coin operator $C_u = 2|s_u\rangle\langle s_u| - I$, with $|s_u\rangle = \frac{1}{\sqrt{d_u}} \sum_{v \in \text{deg}(u)} |v\rangle$. S , the flip-flop shift operator, is defined as $S|uv\rangle = |vu\rangle$, where $|uv\rangle = |u\rangle \otimes |v\rangle$ denotes a particle at vertex u pointing towards vertex v . Given the initial state $|\Psi_0\rangle$, the walker's state after h steps is $|\Psi_h\rangle = U_{\text{walk}}^h |\Psi_0\rangle$.

1.2 The welded tree problem

The welded tree problem was proposed in [17] as a black-box (oracle) problem to show that a quantum algorithm can be exponentially faster than any classical algorithm with the help of CTQW. To achieve exponential *algorithmic* speedup, the graph to be traversed is carefully designed: the welded tree G_n consists of two horizontal-positioned full binary trees of height n with their 2^n leaves in the middle. The root of the left tree is the entrance denoted by s , and the root of the right tree is the exit denoted by t . The leaves in the middle are connected by a *random cycle* that alternates between the leaves of the two trees instead of identifying them in the direct way. (See the dashed line in Fig. 1) This makes the leaves have degree 3 instead of 2, indistinguishable from all the other internal nodes.

The number of vertices in G_n is $|V(G_n)| = 2(2^{n+1} - 1)$, thus $(n + 2)$ -bit string is enough to encode all the vertices. However, to ensure the classical hardness of the problem [17, Lemma 7], each vertex $u \in V(G_n)$ is *randomly* assigned a distinct $2n$ -bit string as its name, except that the entrance is fixed as $s \equiv 0^{2n}$. We retain $\perp \equiv 1^{2n}$ as the special symbol, so that the graph G_n can be specified by an $2^{2n} \times 3$ *adjacency list* Γ (See the table in Fig. 1). Note that when $u \in \{0, 1\}^{2n}$ is the root s or t , exactly one of $\{\Gamma(u, i) : i = 1, 2, 3\}$ is \perp .

The adjacency list Γ is provided in the form of an oracle (black box) O , so that the only way to know about Γ is to query O with a name $u \in \{0, 1\}^{2n}$, and the oracle will output all the items in row u of Γ :

$$O(u) = \{\Gamma(u, i) : i = 1, 2, 3\}. \quad (1)$$

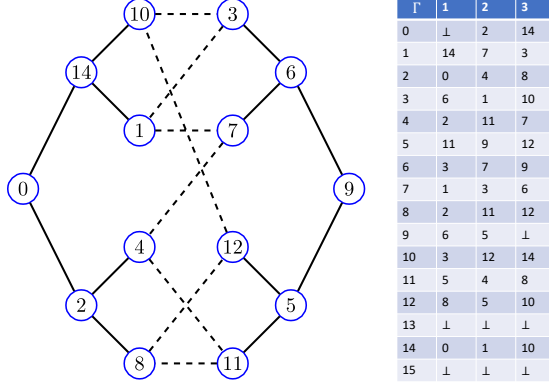


Fig. 1 A welded tree G_n for $n = 2$ and its $2^{2n} \times 3$ adjacency list Γ . $s = 0$ is the entrance and $t = 9 = (1001)_2$ is the exit. The dashed lines in the middle is the random cycle connecting the two trees.

We are concerned with the number of times an algorithm queries the oracle O (a.k.a query complexity) to find the exit name t . In the quantum model, the effect of O is

$$O |u\rangle \bigotimes_{i=1}^3 |v_i\rangle = |u\rangle \bigotimes_{i=1}^3 |v_i \oplus \Gamma(u, i)\rangle, \quad (2)$$

where u, v_i are all $2n$ -bit string and \oplus denotes bit-wise modulo 2 addition. The welded tree problem can now be formally stated as Definition 1.1.

Definition 1.1 (the welded tree problem). *Given the entrance name $s = 0^{2n}$, find the exit name t of the welded tree G_n with as few queries as possible to its adjacency list oracle O .*

Since the degree of each vertex in G_n is no more than 3, even if the quantum oracle O is provided in its weaker form such that it returns only one adjacent vertex $\Gamma(u, i)$ when queried with (u, i) , as is the case in [17], the influence on the query complexity is at most by a constant factor and can be neglected.

1.3 Our contribution

In this paper, we propose a rather succinct quantum algorithm (Algorithm 1 in Section 4) to solve the welded tree problem, which is simply to walk on the welded tree with the operator $U_{\text{walk}} = SC$ from an initial state $|\Psi_s\rangle$ that is constructed from the entrance vertex s . We will show that the coin operator C can be implemented with 4 queries to the given oracle O and the shift operator S has no queries to O . Also, we will prove that after $T \in O(n \log n)$ steps which can be predetermined efficiently on classical computers, the walker reaches the exit vertex t with probability at least $\Omega(\frac{1}{n})$. More exactly, there is $|\langle \Psi_t | U_{\text{walk}}^T | \Psi_s \rangle|^2 > c \frac{1}{n}$ for constant c , where $|\Psi_t\rangle$ encodes the exit t . Therefore, the query complexity of the algorithm is $O(n^2 \log n)$. Furthermore, the algorithm can be improved to a deterministic one with $O(n^{1.5} \log n)$ queries by using deterministic (or exact) amplitude amplification as shown by Algorithm 2

in Section 5. In addition, we conjecture that the actual complexity of our algorithm is $O(n^{4/3})$ (Conjecture 6.1 in Section 6), which is strongly supported by numerical simulation for $n = 6, \dots, 1000$, with the strict proof left as an open problem.

The significance of our results, in our opinion, lies at least in the following two aspects:

1. Our algorithm is rather succinct compared with the one in [20], which not only changes the stereotype that coined quantum walks can only achieve quadratic speedups over classical algorithms, but also demonstrates the power of the simplest quantum walk models.
2. Our algorithm can be made deterministic theoretically, whereas existing methods cannot (see Table 1). Thus, it becomes one of the few examples that exhibits exponential separation between deterministic (exact) quantum and randomized query complexities, and may have potential applications in graph property testing problems [21, 22]. Previous examples of this kind of separation include Simon's problem [23] and its generalization [24]. This deterministic algorithm may also change people's perception that since quantum mechanics is inherently probabilistic, deterministic quantum algorithms with exponential speedups for the welded tree problem are out of the question.

1.4 Technical overview

Despite the succinctness of our algorithms, there are some non-trivial steps in designing and analyzing it, without losing technical challenges:

1. Constructing the operator $U_{\text{walk}} = SC$ from the given oracle O (Lemma 2.1). As the flip-flop shift operator S requires no oracle queries, the key is to construct the coin operator C . Our implementation of C is inspired by [20], but it is much simpler as alternative neighbourhoods technique is not needed in this paper.
2. Reducing the $\Theta(2^n)$ -dimensional state space to a $(4n + 2)$ -dimensional invariant subspace (Lemma 3.1). In this subspace, the operator $U_{\text{walk}} = SC$ takes the form of a $(4n + 2)$ -dimensional square matrix $M_U = M_S M_C$, and the initial state corresponds to the first base vector $|0\rangle$ (whose transpose is $[1, 0, \dots, 0]$) and the target state corresponds to the last base vector $|4n + 1\rangle$ (whose transpose is $[0, \dots, 0, 1]$). The reduction is done by grouping the vertices according to their layers, which is inspired by [17], but since our coined quantum walk is carried out on the edges of the graph, there is some nontrivial difference.
3. Analyzing the success probability, which is probably the most technical step. This is shown in two steps:
 - (i) Obtaining the spectral decomposition of matrix $M_U = \sum_j e^{i\varphi_j} |E_j\rangle \langle E_j|$ (Lemma 4.1). This is inspired by a spectral decomposition result in [25], but we improve it with an observation concerning Chebyshev polynomial of the second kind. The improvements make the equation that the eigenvalues need to satisfy become clear, explicit and easy to analyze.
 - (ii) Instead of directly considering a fixed iteration number t (the difficulty of this approach is noted in Remark 4.4), we will prove that the average success probability $\mathbb{E} | \langle 4n + 1 | M_U^t | 0 \rangle |^2$ has a $\Omega(\frac{1}{n})$ lower bound when t is chosen according

to a specific distribution over $\{0, 1, \dots, O(n \log n)\}$. A key component of the proof is the helper Lemma 4.2 (inspired by [26, Lemma 3]), which relates the lower bound of $\mathbb{E} |\langle 4n + 1 | M_U^t | 0 \rangle|^2$ with, roughly speaking, the first and last component of eigenvector $|E_j\rangle$ and the characteristic of eigenvalue angles φ_j . Thus, the spectral decomposition $M_U = \sum_j e^{i\varphi_j} |E_j\rangle \langle E_j|$ in step (i) is of crucial importance.

1.5 Related work

The original algorithm proposed by Childs et al. [17] is based on CTQW and they prove that the CTQW will find the exit with probability $\Omega(1/n)$ at a time of $O(n^4)$. They also showed that the CTQW e^{iHt} can be simulated for time t with $O(t^2)$ oracle queries. Thus combined with fixed-point amplitude amplification [27, 28], the overall query complexity is $O(n^{8.5})$, where $n^{8.5} = n^{1/2} \cdot n^{4.2}$. Lately it was improved to $O(n^{2.5} \log^2 n)$ [26]. In contrast, any classical algorithm requires $2^{\Omega(n)}$ queries [17, 29]. It was claimed in [30] that there exist exponential algorithmic speedups based on DTQW for the welded tree problem, but no explicit algorithm was given there. Recently, a quantum algorithm based on the multidimensional quantum walk framework was proposed by Jeffery and Zur [20], solving the problem with $O(n)$ queries and $O(n^2)$ time complexity. The framework uses phase estimation [31] to gain one-bit information about the exit name, and then uses the Bernstein-Vazirani algorithm [32] to obtain the whole name. We summarize previous results on the welded tree problem in Table 1.

Table 1 Summary of previous work on the welded tree problem.

algorithmic type	queries	succinct?	deterministic?
classical [17, 29]	$2^{\Omega(n)}$		*1
CTQW [17]	$O(n^{8.5})$	Yes	No
CTQW [26]	$O(n^{2.5} \log^2 n)$	Yes	No
DTQW [20]	$O(n)$	No	No
DTQW, this work	$O(n^{1.5} \log n)$	Yes	Yes

¹The lower bound holds for any classical randomized algorithm and thus also holds for deterministic algorithm.

Compared to the recent quantum algorithm based on multidimensional quantum walks [20], our algorithm has the following advantages:

1. Succinct algorithmic procedure. Our algorithm (see Algorithm 1) simply iterates the coined quantum walk operator U_{walk} for a predetermined time T and then measure the first register to obtain the result. In contrast, [20] has to combine with Bernstein-Vazirani algorithm [32] in order to learn the whole name, because their multidimensional quantum walk framework using phase estimation can only obtain one-bit information about the exit name (which corresponds to the inner-product oracle in BV algorithm).
2. Simpler implementation of the quantum walk operator. Our implementation of U_{walk} is simpler as the coin operator C can be easily implemented with two oracle

queries and the shift operator S is merely $2n$ parallel SWAP gates. In contrast, it was said in [20, Remark 4.8] that one has to carefully assign different weights to the graph's edges in order to balance between the positive and negative witness size, so that the polynomial query complexity is possible. The weight assigning scheme makes the implementation of the quantum walk operator much more complicated: (i) The alternative neighbourhoods technique has to be used since the oracle does not provide information about which neighbouring vertex is closer to the root. The technique works as follows: instead of reflecting around the uniform superposition of neighbours (which is what our coin operator C does), one has to reflect around a subspace spanned by some easily preparable states. This makes the operator's implementation more complicated. (ii) Due to the specific weight assigning scheme, one has to handle separately the cases when n is odd or even, and determine the parity of the layers at which each vertex lies, and also assign different weight $w_0 = w_M = 1/(cn)$ to the edges $(s, \perp), (t, \perp)$.

3. Certainty of success theoretically. Since the multidimensional framework [20] uses phase estimation which is intrinsically randomized, it cannot be made deterministic, but our simple coined quantum walk algorithm can be made deterministic theoretically (Algorithm 2).

Compared to the algorithms based on CTQW [17, 26], our algorithms has a better query complexity, and can be adapted to succeed with certainty. On the contrary, the implementation of the CTQW operator e^{iHt} from oracle O involves the use of linear combination tool in Hamiltonian simulation, thus error is introduced inevitably. Also, choosing the quantum walk time t according to some distribution leads to additional randomness.

1.6 Paper organization

The rest of the paper is organized as follows. In Section 2 we define the coined quantum walk operator U_{walk} and give a detailed implementation of U_{walk} from the quantum oracle O . In Section 3 we reduce the full state space to a $(4n+2)$ -dimensional invariant subspace and deduce the reduced matrix M_U , which lays an important first step for the correctness and complexity analysis of our algorithms. In Section 4 we present a succinct algorithm (Algorithm 1) and prove a rigorous query upper bound. In Section 5 we present the theoretically deterministic algorithm (Algorithm 2). Numerical simulation is shown in Section 6 indicating that the actual performance of our algorithms is better. We conclude this paper in Section 7.

2 Implementing the coined quantum walk operator

As the adjacency list Γ of the welded tree G_n defined in Section 1.2 is unknown and can only be accessed through the oracle O , the implementation of the coined quantum walk operator U_{walk} on G_n needs some careful design as presented in this section.

First, the state space of the coined quantum walk is:

$$\mathcal{H} = \text{span}\{|u\rangle_{r_1} |v\rangle_{r_2} : u, v \in \{0, 1\}^{2n}\}, \quad (3)$$

which is the state space of $4n$ qubits. The subscript r_i of the two registers will serve later for the convenience of describing the construction of

$$U_{\text{walk}} = SC. \quad (4)$$

Let $\varphi(u) = \frac{1}{\sqrt{3}} \sum_{i=1}^3 |\Gamma(u, i)\rangle$ be the uniform superposition of the adjacent vertices of u and let $C_u = 2|\varphi(u)\rangle\langle\varphi(u)| - I$. Then the coin operator C is given by

$$C = \sum_{u \in \{0,1\}^{2n}} |u\rangle\langle u| \otimes C_u \quad (5)$$

$$= 2 \sum_{u \in \{0,1\}^{2n}} |u, \varphi(u)\rangle\langle u, \varphi(u)| - I. \quad (6)$$

Note that we allow the sum to include $u \notin V(G_n)$, so that the implementation of Ref_\perp (see Eq. (12)) does not need to check whether u is indeed a vertex in G_n or not. When $r \in \{s, t\}$ and $\Gamma(r, i_1) = \perp$, we let

$$\varphi(r) = \frac{1}{\sqrt{2}}(|\Gamma(r, i_2)\rangle + |\Gamma(r, i_3)\rangle), \quad (7)$$

reflecting the fact that $r \rightarrow \perp$ is not an edge in the graph.

The shift operator S is the SWAP operator on the vertex pair $\{u, v\}$:

$$S = \sum_{u, v \in \{0,1\}^{2n}} |v, u\rangle\langle u, v|, \quad (8)$$

which is actually a reflection operator as well:

$$S = 2 \sum_{u \leq v} |\psi_{u,v}\rangle\langle\psi_{u,v}| - I, \quad (9)$$

where

$$|\psi_{u,v}\rangle = \begin{cases} \frac{|u,v\rangle + |v,u\rangle}{\sqrt{2}}, & u < v; \\ |u, v\rangle, & u = v. \end{cases} \quad (10)$$

Lemma 2.1. *The coined quantum walk operator $U_{\text{walk}} = SC$ can be implemented with 2 oracle queries and $O(n)$ elementary operations.*

Proof. First, the implementation of S is quite simple, just apply the SWAP gate to the corresponding $2n$ pairs of qubits between registers r_1 and r_2 , which takes $O(n)$ basic operations. The implementation of C is more complicated and requires 2 oracle queries as shown below.

We implement C in two steps: first to construct a unitary operator U_φ that has the following effect

$$U_\varphi : |u, \perp\rangle \mapsto |u, \varphi(u)\rangle, \quad (11)$$

and then to construct the reflection

$$\text{Ref}_\perp = 2 \sum_{u \in \{0,1\}^{2n}} |u, \perp\rangle \langle u, \perp| - I = I_{r_1} \otimes (2|\perp\rangle \langle \perp| - I_{r_2}). \quad (12)$$

Thus, we have

$$C = U_\varphi \text{Ref}_\perp U_\varphi^\dagger, \quad (13)$$

where U_φ^\dagger can be implemented by executing the conjugate of quantum gates composing U_φ in reverse order.

As global phase shift can be neglected, we will implement $-\text{Ref}_\perp$. Observe that $-\text{Ref}_\perp$ simply adds a relative phase shift of (-1) to $|v\rangle_{r_2}$ when $v = \perp = 1^{2n}$. Thus, using phase kick-back effect, $-\text{Ref}_\perp$ can be easily constructed by flipping an auxiliary qubit register $|-\rangle$ conditioned on all the $2n$ qubits in register r_2 being in state $|1\rangle$ (i.e. apply a $C^{2n} - \text{NOT}$ gate, *which decomposes to $O(n)$ basic gates*).

The implementation of U_φ requires 2 oracle queries and $O(n)$ basic operations, which is a bit lengthy due to the special handling of $\varphi(r)$ (Eq. (7)) and is thus deferred to Appendix A. Note that Ref_\perp is carried out on register r_2 and leaves register r_1 unchanged, so the 2 oracle queries in U_φ and U_φ^\dagger closest to Ref_\perp in $C = U_\varphi \text{Ref}_\perp U_\varphi^\dagger$ is cancelled out. Thus C can be implemented with 2 oracle queries.

As can be seen from the italics, the implementation of U_{walk} takes $O(n)$ basic operations in total. \square

Remark 2.1. *If we enable the oracle to return all the neighbours coherently, i.e. $O : |u, \perp\rangle \mapsto |u, \varphi(u)\rangle$, which is a common assumption in the Markov chain based DTQW framework, then the implementation of U_φ shown above is unnecessary. But if this is the case, we will need an additional oracle to check if u is the exit.*

The initial state of the coined quantum walk is

$$|s, \varphi(s)\rangle = \frac{1}{\sqrt{2}}(|\Gamma(s, i_2)\rangle + |\Gamma(s, i_3)\rangle), \quad (14)$$

which can be obtained with 2 oracle queries from $|s, \perp\rangle$ similar to step 4 in Appendix A. We denote this state preparation unitary by

$$U_p : |s, \perp\rangle \mapsto |s, \varphi(s)\rangle. \quad (15)$$

3 Reducing to the low-dimensional invariant subspace

In this section, we will determine the $(4n + 2)$ -dimensional invariant subspace \mathcal{H}_0 of the coined quantum walk operator U_{walk} based on layers of vertices in G_n , so that the amplitude on the target state $|t, \varphi(t)\rangle$ after applying U_{walk}^T to the initial state $|s, \varphi(s)\rangle$ can be calculated exactly when n is fixed, regardless of the vertices' random naming

or the random cycle in the middle of G_n . This lays an important first step for the correctness and complexity analysis of our algorithms.

Specifically, we have the following lemma.

Lemma 3.1. *The coined quantum walk operator U_{walk} for the welded tree G_n has a $(4n + 2)$ -dimensional invariant subspace*

$$\mathcal{H}_0 = \text{span}\{|0, R\rangle, |1, L\rangle, |1, R\rangle, \dots, |2n, L\rangle, |2n, R\rangle, |2n + 1, L\rangle\}, \quad (16)$$

where $|0, R\rangle = |s, \varphi(s)\rangle$ is the initial state, $|2n + 1, L\rangle = |t, \varphi(t)\rangle$ is the target state, and the other states $|k, L\rangle, |k, R\rangle$ are defined respectively in Eqs. (17) (18) for $k = 1 \sim n$ in the left tree, and similarly for $k = (n + 1) \sim 2n$ in the right tree. In this basis, the coined quantum walk operator U_{walk} can be represented by a $(4n + 2)$ -dimensional square matrix $M_U = M_S \cdot M_C$, where M_C and M_S are shown in Eqs. (22), (24) respectively.

Proof. The welded tree G_n has $2(n + 1)$ layers of vertices, and we denote by V_k the set of vertices in the k -th layer. Thus in the left tree, $|V_k| = 2^k$ for $k \in \{0, 1, \dots, n\}$; and in the right tree, $|V_{n+k}| = 2^{n+1-k}$ for $k \in \{1, 2, \dots, n + 1\}$. The two basis states $|k, L\rangle, |k, R\rangle$ with $k \in \{1, \dots, n\}$ of \mathcal{H}_0 are related to V_k in the left tree, and are defined as the superpositions of the directed edges pointing to the root and to the random cycle, respectively:

$$|k, L\rangle := \frac{1}{\sqrt{2^k}} \sum_{u \in V_k} |u, \Gamma(u, i_1)\rangle \quad (17)$$

where $\Gamma(u, i_1)$ is the adjacent vertex of u closest to the root s , and

$$|k, R\rangle := \frac{1}{\sqrt{2^k}} \sum_{u \in V_k} \frac{1}{\sqrt{2}} (|u, \Gamma(u, i_2)\rangle + |\Gamma(u, i_3)\rangle). \quad (18)$$

Note that the composing computational basis states of $|k, L\rangle, |k, R\rangle$ with $k \in \{1, \dots, n\}$ are all distinct, since they represent different directed edges in the welded tree graph. Thus these basis states are mutually orthogonal. The two basis states $|n + k, L\rangle, |n + k, R\rangle$ with $k \in \{1, \dots, n\}$ related to V_{n+k} in the right tree are defined similarly. Note that $|0, R\rangle := |s, \varphi(s)\rangle$ is the initial state and $|2n + 1, L\rangle := |t, \varphi(t)\rangle$ is the target state. Note also that there is no $|0, R\rangle$ or $|2n + 1, L\rangle$. A diagram of the $4n + 4 = 12$ basis states of \mathcal{H}_0 when $n = 2$ is shown in Fig. 2.

Observe that

$$|u, \varphi(u)\rangle = \sqrt{\frac{1}{3}} |u, \Gamma(u, i_1)\rangle + \sqrt{\frac{2}{3}} \frac{1}{\sqrt{2}} (|u, \Gamma(u, i_2)\rangle + |\Gamma(u, i_3)\rangle). \quad (19)$$

Thus by the definition of the coin operator C (Eq. (6)) and linearity, the 2-dimensional subspace spanned by $\{|k, L\rangle, |k, R\rangle\}$ is invariant under C , and the matrix expression

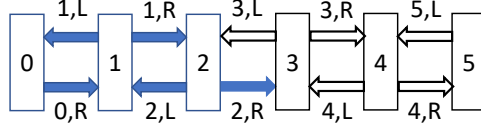


Fig. 2 Diagram of the basis states of the reduced coined quantum walk subspace \mathcal{H}_0 when $n = 2$. The box with number inside represents the vertex set V_k of the k -th layer. The solid blue arrows represent basis states $|k, L\rangle, |k, R\rangle$ related to V_k with $k \in \{1, \dots, n\}$ in the left tree, and the black hollow arrows represent basis states $|n+k, L\rangle, |n+k, R\rangle$ related to V_{n+k} with $k \in \{1, 2, \dots, n\}$ in the right tree. The state $|0, R\rangle := |s, \varphi(s)\rangle$ and $|2n+1, L\rangle := |t, \varphi(t)\rangle$ are the initial and target states respectively.

of C in this basis is

$$R_A := 2 \begin{bmatrix} \sqrt{\frac{1}{3}} \\ \sqrt{\frac{2}{3}} \end{bmatrix} \cdot \left[\sqrt{\frac{1}{3}}, \sqrt{\frac{2}{3}} \right] - I = \begin{bmatrix} -\frac{1}{3} & \frac{2\sqrt{2}}{3} \\ \frac{2\sqrt{2}}{3} & \frac{1}{3} \end{bmatrix}. \quad (20)$$

Similarly, the matrix expression of C in the basis $\{|n+k, L\rangle, |n+k, R\rangle\}$ related to V_{n+k} in the right tree is

$$R'_A := 2 \begin{bmatrix} \sqrt{\frac{2}{3}} \\ \sqrt{\frac{1}{3}} \end{bmatrix} \cdot \left[\sqrt{\frac{2}{3}}, \sqrt{\frac{1}{3}} \right] - I = \begin{bmatrix} \frac{1}{3} & \frac{2\sqrt{2}}{3} \\ \frac{2\sqrt{2}}{3} & -\frac{1}{3} \end{bmatrix}. \quad (21)$$

Note that $|0, R\rangle$ and $|2n+1, L\rangle$ are invariant under C by Eq. (7). Thus the matrix expression of C in the basis $\{|0, R\rangle, |1, L\rangle, |1, R\rangle, \dots, |2n, L\rangle, |2n, R\rangle, |2n+1, L\rangle\}$ is

$$M_C := \text{diag}(1, \underbrace{R_A, \dots, R_A}_n, \underbrace{R'_A, \dots, R'_A}_n, 1). \quad (22)$$

Note that $|k, R\rangle$ and $|k+1, L\rangle$ with $k \in \{0, \dots, 2n\}$ are equal superpositions of basis states in $\{|u, v\rangle : u \in V_k, v \in V_{k+1}\}$ and $\{|v, u\rangle : u \in V_k, v \in V_{k+1}\}$ respectively, which represent the same set of edges but the direction are all reversed. Recall that the shift operator S swaps ‘directed edge’ $|u, v\rangle$ with $|v, u\rangle$, therefore by linearity S simply swaps $|k, R\rangle$ with $|k+1, L\rangle$, and the 2-dimensional subspace spanned by $\{|k, R\rangle, |k+1, L\rangle\}$ is invariant under S . The matrix expression of S in this two basis states is

$$R_B := \begin{bmatrix} 0 & 1 \\ 1 & 0 \end{bmatrix} = 2|+\rangle\langle+| - I. \quad (23)$$

Thus, the matrix of S in the basis $\{|0, R\rangle, |1, L\rangle, |1, R\rangle, \dots, |2n, L\rangle, |2n, R\rangle, |2n+1, L\rangle\}$ is

$$M_S := \text{diag}(\underbrace{R_B, \dots, R_B}_{2n+1}). \quad (24)$$

As a result, the operator U_{walk} corresponds to a $(4n + 2)$ -dimensional square matrix

$$M_U = M_S \cdot M_C. \quad (25)$$

In addition, the initial state $|0, R\rangle := |s, \varphi(s)\rangle$ corresponds to the $(4n + 2)$ -dimensional vector $|0\rangle = [1, 0, \dots, 0]^T$, and the target state $|2n + 1, L\rangle := |t, \varphi(t)\rangle$ corresponds to $|4n + 1\rangle = [0, 0, \dots, 1]^T$. \square

4 Succinct quantum algorithm with $O(n^2 \log n)$ queries

Here we present a rather succinct quantum algorithm (i.e., Algorithm 1) for the welded tree problem, which is to first efficiently compute a walk step number T_1 on classical computers, and then simply perform the walk operator U_{walk} with T_1 times. The correctness is guaranteed by Theorem 4.1, from which together with Lemma 2.1 it is easy to see that the query complexity of Algorithm 1 is $O(n^2 \log n)$, with an additional time complexity of $O(n \cdot n^2 \log(n)) = O(n^3 \log(n))$.

Algorithm 1 succinct quantum algorithm for the welded tree problem

Input: adjacency list quantum oracle O (see Eq. (2)) for the welded tree G_n , and the entrance name $s \equiv 0^{2n}$.

Output: the exit name t .

Procedure:

1. Classically predetermine the walk step number T_1 : For the initial vector $|\psi_0\rangle = |0\rangle$, loop “ $|\psi_T\rangle \leftarrow M_U |\psi_{T-1}\rangle$ ” (see Eq. (25) for M_U) and “ $p_T \leftarrow |\langle 4n + 1 | \psi_T \rangle|^2$ ”, stop when $T > 3.6 n \log(24n)$. Record the *largest* p_{T_1} for $2n < T_1 < 3.6 n \log(24n)$ and the corresponding T_1 .
 2. Quantum walk: Apply T_1 steps of coined quantum walk, i.e. $U_{\text{walk}}^{T_1}$ (Eq. (4)) to the initial state $|s, \varphi(s)\rangle$ (Eq. (14)) and measure the first register in the computational basis to obtain the exit name with $\Omega(\frac{1}{n})$ probability.
 3. Classical repetition: Repeat step 2 for $O(n)$ times to obtain the exit name t with constant probability.
-

Theorem 4.1. *Consider the success probability $p(t) := |\langle 4n + 1 | M_U^t |0\rangle|^2$, where M_U is defined by Eq. (25). Then for sufficiently large n and $T \approx 3.6 n \log(24n)$, we have*

$$\max\{p(t) : t \in [2n, T]\} > \frac{1}{24n}. \quad (26)$$

The remainder of this section is to prove the above theorem. As mentioned in Section 1.4, the first and most important step to prove Theorem 4.1 is to obtain the spectral decomposition of the reduced matrix, i.e. $M_U = \sum_j e^{i\varphi_j} |E_j\rangle \langle E_j|$, which will be shown by Lemma 4.1 in Section 4.1. Then we will present and prove the helper

Lemma 4.2 in Section 4.2, a key step in obtaining the lower bound $\Omega(\frac{1}{n})$ of the average success probability $\mathbb{E}|\langle 4n+1 | M_U^t | 0 \rangle|^2$, from which Theorem 4.1 follows. In order to use this helper lemma, we will need the values $\langle 4n+1 | E_j \rangle \cdot \langle E_j | 0 \rangle$ for $j \in S$, and bound the gap $\Delta E_S = \min\{|\varphi_j - \varphi_k| : \varphi_j \in S, \varphi_k \in E, k \neq j\}$ by choosing $S \subseteq E = \{\varphi_j\}$ well (so that ΔE_S will be of order $\Omega(\frac{1}{n})$ as shown by Eq. (58) and Lemma 4.4 in Section 4.3). Thus, even though the explicit formula shown in Lemma 4.1 is quite complicated, we only need to pay attention to the the first and last term of the eigenvectors $|E_j\rangle$, and the gap between the eigenvalue angles φ_j .

4.1 Spectral decomposition of M_U

As a preliminary, first notice that M_C (see Eq. (22)) can be expressed as $2AA^\dagger - I$, where A is the following $2(2n+1) \times 2(n+1)$ centrosymmetric matrix:

$$A = \left[\begin{array}{c|c} 1 & \\ \sqrt{p} & \\ \sqrt{q} & \\ & \ddots \\ & & \sqrt{p} \\ & & \sqrt{q} \\ \hline & & & & * \end{array} \right], \quad (27)$$

where

$$p = \frac{1}{3}, \quad q = 1 - p \quad (28)$$

represent respectively the probability of walking to the roots and to the random cycle. The $(2n+1) \times (n+1)$ sub-matrix in the bottom right-hand corner denoted by ‘*’ can be deduced from the centrosymmetry of A . It’s easy to see that all the columns in A are orthonormal, thus $A^\dagger A = I_{2(n+1)}$.

Lemma 4.1. *The matrix M_U defined by Eq. (25) has $(4n+2)$ different eigenvalues. Two of which are ± 1 , and the respective eigenvectors are $|u_{\pm 1}\rangle = A|v_{\pm 1}\rangle$, where the i -th component of $|v_{\pm 1}\rangle$ denoted by $v_{\pm 1}(i)$ is shown in the following:*

$$v_{\pm 1}(i) = \begin{cases} 1, & i = 1, \\ (\pm\sqrt{q/p})^{i-1}/\sqrt{q}, & i = 2 \sim n+1, \\ \pm(*) & i = n+2 \sim 2n+2. \end{cases} \quad (29)$$

The (*) above can be deduced from centrosymmetry of $|v_{\pm 1}\rangle$. The square of norms are:

$$\| |u_{\pm 1}\rangle \|^2 = \| |v_{\pm 1}\rangle \|^2 = \frac{2}{p-q} \{2p - (q/p)^n\}. \quad (30)$$

The other $4n$ eigenvalues are $\exp(\pm i\varphi_{\pm k})$ with $k = 2 \sim n+1$, where $\varphi_{\pm k} = \arccos \lambda_{\pm k}$ and $\lambda_{-k} = -\lambda_k$. Here, $\lambda_{\pm k} = 2\sqrt{pq} \cos \theta_{\pm k}$, and $\theta_{\pm k}$ ($\theta_{-k} := \pi - \theta_k$) are

the $2n$ roots of the following equation:

$$\sqrt{q} \sin(n+1)\theta \pm \sqrt{p} \sin n\theta = 0. \quad (31)$$

The eigenvectors corresponding to $\exp(\pm i\varphi_{\pm k})$ are:

$$|u_{\pm, \pm k}\rangle := |a_{\pm k}\rangle - \exp(\pm i\varphi_{\pm k}) |b_{\pm k}\rangle, \quad (32)$$

where $|a_{\pm k}\rangle = A |v_{\pm k}\rangle$, $|b_{\pm k}\rangle = M_S |a_{\pm k}\rangle$. The components of $|v_{\pm k}\rangle$ are as follows:

$$v_{\pm k}(i) = \begin{cases} 1, & i = 1, \\ \frac{\lambda_{\pm k}}{\sqrt{p}} U_{i-2}(\lambda_{\pm k}/\sqrt{pq}) - \frac{1}{\sqrt{q}} U_{i-3}(\lambda_{\pm k}/\sqrt{pq}), & i = 2 \sim n+1 \\ \pm(*), & i = n+2 \sim 2n+2 \end{cases} \quad (33)$$

where $(*)$ can be deduced from centrosymmetry, and $U_i(x)$ is the monic Chebyshev of the second kind:

$$U_i(x) = \frac{\sin(i+1) \arccos \frac{x}{2}}{\sqrt{1 - (\frac{x}{2})^2}}. \quad (34)$$

The square of norms are

$$\| |u_{\pm, \pm k}\rangle \|^2 = \frac{2(1 - \lambda_k^2)^2}{q \sin^2 \theta_k} \left(n + \sqrt{\frac{q}{p}} \frac{\sin((n+1)2\theta_k)}{2 \sin \theta_k} \right). \quad (35)$$

Proof. The proof is a bit lengthy and is deferred to Appendix B. \square

Remark 4.1. We suspect the reason that no succinct algorithm for the welded tree problem based on simple coined quantum walks has been proposed a priori, is that an enough understanding on the spectral decomposition of the DTQW operator has not been obtained before. Although Ref. [25] is a big step towards this direction, the results obtained there are not satisfactory:

$$\frac{1}{T} \sum_{t \in [T]} |\langle 4n+1 | M_U^t | 0 \rangle|^2 = 2^{-\Omega(n)}, \quad T \rightarrow \infty, \quad (36)$$

showing that the average success probability is exponentially small when $T \rightarrow \infty$.

4.2 The helper lemma

Another key component in proving Theorem 4.1 is the following helper Lemma 4.2, which is a discrete-time adaptation of [26, Lemma 3]. However, our proof of Lemma 4.2 is simpler than the one for [26, Lemma 3], as it does not involve integral or characteristic functions of continuous random variables. Moreover, their intermediate step [26, Lemma 4] considers the Frobenius norm of the difference between density matrices, which introduces a strange factor of $\sqrt{3}$.

Lemma 4.2 shows that when the iteration number t is chosen according to some specific distribution on $[T] := \{0, 1, \dots, T-1\}$, the average success probability has a

lower bound that is related to the characteristic of the eigenvalue angles of M_U and the products of the first and the last term of the eigenvectors.

Lemma 4.2. *Assume that M_U has a spectral decomposition $M_U = \sum_j e^{i\varphi_j} |E_j\rangle \langle E_j|$ where φ_j are all distinct, and the initial state is written in this eigenbasis as $|\psi_0\rangle = \sum_j c_j |E_j\rangle$ and the target state as $|y\rangle = \sum_j y_j |E_j\rangle$. For a subset $S \subseteq E := \{\varphi_j\}$, denote $\Delta E_S := \min\{|\varphi_j - \varphi_k| : \varphi_j \in S, \varphi_k \in E, k \neq j\}$. Let $t = \sum_{m=1}^k t_m$ be the sum of k i.i.d. uniform random variables $t_m \in [T]$. Consider the average success probability*

$$\bar{p}(y|\psi_0) = \frac{1}{T^k} \sum_{t \in [T]^k} |\langle y | M_U^t | \psi_0 \rangle|^2, \quad (37)$$

where t can be regarded as a random vector $(t_1, t_2, \dots, t_k) \in [T]^k$ each with equal probability $\frac{1}{T^k}$. Then $\bar{p}(y|\psi_0)$ has the following lower bound:

$$\bar{p}(y|\psi_0) \geq \sum_{j:\varphi_j \in S} |y_j^* c_j|^2 - \left(\frac{\pi}{T \Delta E_S} \right)^k. \quad (38)$$

Proof. Denote by $A(t) := \langle y | M_U^t | \psi_0 \rangle$ the amplitude of success, then according to the spectral decomposition of M_U , we have $A(t) = \sum_j y_j^* c_j e^{i\varphi_j t}$. From $|A(t)|^2 = A(t)A(t)^*$, we know

$$\bar{p}(y|\psi_0) = \sum_{j,j'} \left[y_j^* c_j y_{j'}^* c_{j'} \sum_{t \in [T]^k} \frac{1}{T^k} e^{i(\varphi_j - \varphi_{j'})t} \right]. \quad (39)$$

We now divide the sum $\sum_{j,j'}[\dots]$ in Eq. (39) into the following three parts.

1. $j = j'$ and $\varphi_j \in S$: $\sum_{j,j'}[\dots] = \sum_{j \in S} |y_j^* c_j|^2$.
2. $\varphi_j \notin S$ and $\varphi_{j'} \notin S$:

$$\sum_{j,j'}[\dots] = \frac{1}{T^k} \sum_t \sum_j y_j^* c_j e^{i\varphi_j t} \sum_{j'} y_{j'}^* c_{j'}^* e^{-i\varphi_{j'} t} \geq 0. \quad (40)$$

3. The rest part, i.e. $j \neq j'$, $\varphi_j \in S, \varphi_{j'} \in S$, or $\varphi_j \notin S, \varphi_{j'} \in S$, or $\varphi_j \in S, \varphi_{j'} \notin S$.

Therefore, we only need to prove that the value of part (3) is greater than $-\left(\frac{\pi}{T \Delta E_S}\right)^k$.

We do this by showing that its absolute value is less than $\left(\frac{\pi}{T \Delta E_S}\right)^k$. First, note that now $\varphi_j \neq \varphi_{j'}$ and one of them belongs to S . Thus $|\varphi_j - \varphi_{j'}| \geq \Delta E_S$, and we have

$$\left| \sum_{t \in [T]^k} \frac{1}{T^k} e^{i(\varphi_j - \varphi_{j'})t} \right| = \left| \prod_{m=1}^k \sum_{t_m=0}^{T-1} \frac{1}{T} e^{i(\varphi_j - \varphi_{j'})t_m} \right| \quad (41)$$

$$= \prod_{m=1}^k \left| \sum_{t_m=0}^{T-1} \frac{1}{T} e^{i(\varphi_j - \varphi_{j'}) t_m} \right| \quad (42)$$

$$= \left| \frac{1 - e^{i(\varphi_j - \varphi_{j'}) T}}{T(1 - e^{i(\varphi_j - \varphi_{j'})})} \right|^k \quad (43)$$

$$\leq \left(\frac{2}{T \cdot 2\Delta E_S / \pi} \right)^k = \left(\frac{\pi}{T\Delta E_S} \right)^k, \quad (44)$$

where we have used $t = \sum_{m=1}^k t_m$ in the first equality, and the following identities $|1 - e^{i\varphi}| = |e^{i\varphi/2} - e^{-i\varphi/2}| = |2 \sin \varphi/2| \geq 2 \frac{\varphi}{\pi}$ in the last line. Then, we can bound the value of part (3) using Cauchy-Schwartz as follows:

$$\left| \sum_{j,j'} [\dots] \right| \leq \left(\frac{\pi}{T\Delta E_S} \right)^k \sum_{j,j'} |y_j^* c_j y_{j'} c_{j'}^*| \quad (45)$$

$$\leq \left(\frac{\pi}{T\Delta E_S} \right)^k \sqrt{\sum_{j,j'} |y_j|^2 |y_{j'}|^2} \sqrt{\sum_{j,j'} |c_j|^2 |c_{j'}|^2} \quad (46)$$

$$= \left(\frac{\pi}{T\Delta E_S} \right)^k. \quad (47)$$

□

Remark 4.2. Lemma 4.2 can be generalized to the case when M_U has multiple eigenangles with the same value, i.e. $M_U = \sum_j e^{i\varphi_j} \Pi_j$, where Π_j denotes the orthogonal projection onto the eigenspace corresponding to $\varphi_j \in E$, and E is the set of all the different eigenangles. In this case, Eq. (38) becomes

$$\bar{p}(y|\psi_0) \geq \sum_{\varphi_j \in S} |\langle y | \Pi_{\varphi_j} | \psi_0 \rangle|^2 - \left(\frac{\pi}{T\Delta E_S} \right)^k. \quad (48)$$

The proof is almost the same, but to bound the absolute value of part (3), we instead use the following arguments:

$$\sum_{(j,j') \in (3)} |\langle y | \Pi_j | \psi_0 \rangle \langle \psi_0 | \Pi_{j'} | y \rangle| \quad (49)$$

$$\leq \sum_{(j,j') \in (3)} \|\Pi_j | y \rangle\| \cdot \|\Pi_j | \psi_0 \rangle\| \cdot \|\Pi_{j'} | \psi_0 \rangle\| \cdot \|\Pi_{j'} | y \rangle\| \quad (50)$$

$$\leq \sqrt{\sum_{j,j'} \|\Pi_j | y \rangle\|^2 \|\Pi_{j'} | y \rangle\|^2} \sqrt{\sum_{j,j'} \|\Pi_j | \psi_0 \rangle\|^2 \|\Pi_{j'} | \psi_0 \rangle\|^2} \quad (51)$$

$$= 1. \quad (52)$$

For an intuitive understanding of Eq. (59), its LHS for $n = 8$ and the horizontal lines $y = 0, \pm \frac{1}{\sqrt{2}}$ are plotted in Fig. 5.

We now present Lemma 4.4 showing that $\Delta_\theta = \Omega(1/n)$ with our choice of S' .

Lemma 4.3. *When n is sufficiently large, the minimal gap Δ_θ of the roots of Eq. (59) has the following $\Omega(1/n)$ lower bound with $S' = (\frac{\pi}{3}, \frac{2\pi}{3})$:*

$$\Delta_\theta = \min\{|\theta_{\pm k} - \theta_{\pm j}| : \theta_{\pm k} \in S', \theta_{\pm j} \in (0, \pi), k \neq j\} \quad (53)$$

$$\geq \frac{\pi - 2\theta_0}{n} \approx \frac{0.15\pi}{n}, \quad (54)$$

where $\tan \theta_0 = \frac{\sqrt{3}}{\sqrt{2}-1}$.

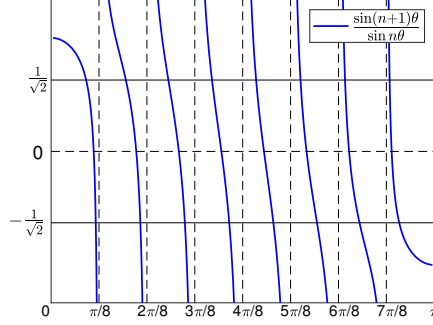


Fig. 3 Left hand side of Eq. (59) for $n = 8$.

4.3 Lower bounding ΔE_S

With Lemma 4.2 in hand, in order to prove Theorem 4.1, we will need to select a suitable subset of eigenvalue angles S and an upper bound of iteration times $T' = k(T-1) < kT$ such that the first term of Eq. (38) is $\Omega(\frac{1}{n})$, and the second term is a smaller $O(\frac{1}{n})$ term.

We now select the eigenvalue angle subset S in Lemma 4.2 to be those $\varphi_{\pm k} = g(\theta_{\pm k})$ whose $\theta_{\pm k} \in S' := (\frac{\pi}{3}, \frac{2\pi}{3})$, where g is the following function:

$$g(\theta_{\pm k}) := \arccos(2\sqrt{pq} \cos \theta_{\pm k}). \quad (55)$$

Note that $g(\theta) \in [\arccos(2\sqrt{pq}), \pi - \arccos(2\sqrt{pq})]$ when $\theta \in [0, \pi]$. Thus the angles $\varphi_{\pm k}$ with $k = 2 \sim (n+1)$ have a constant gap with $\varphi_{\pm 1} = 0, \pi$. Furthermore, it can be seen from Fig. 4 that $g(\theta)$ is monotone increasing on $(0, \pi)$, and the minimal derivative when $\theta \in S'$ is $g'(\pi/3) = \sqrt{6/7}$, since

$$g'(\theta) = \frac{2\sqrt{pq} \sin \theta}{\sqrt{1 - 4pq \cos^2 \theta}}. \quad (56)$$

The minimal angle gap

$$\Delta_\theta := \min\{|\theta_{\pm k} - \theta_{\pm j}| : \theta_{\pm k} \in S', \theta_{\pm j} \in (0, \pi), k \neq j\} \quad (57)$$

of θ_k will result in the minimal angle gap of φ_k to satisfy:

$$\Delta E_S \geq \sqrt{6/7} \Delta_\theta, \quad (58)$$

when n is sufficiently large. This is because we only need to consider the gap between $\theta_{\pm k}$ and $\theta_{\pm j}$ all belonging to S' , and the gap $\overline{\Delta}_\theta$ between $\theta_{\pm k} \in S'$ nearest to $\pi/3$ and its adjacent $\theta_{\pm j}$ on the left. In the latter case, we have $g(\theta_{\pm k}) - g(\theta_{\pm j}) \geq g'(\pi/3 - \overline{\Delta}_\theta) \overline{\Delta}_\theta$. But as $g'(\pi/3 - \overline{\Delta}_\theta) \rightarrow g'(\pi/3)$ when $n \rightarrow \infty$, Eq. (58) holds when n is sufficiently large. Therefore, in order to bound ΔE_S , it's sufficient to consider Δ_θ .

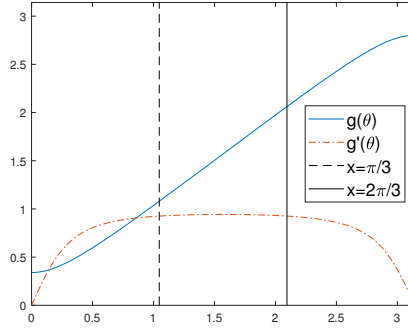


Fig. 4 The function $\varphi = g(\theta)$ defined in Eq. (55), and its derivative $g'(\theta)$.

Eq. (31) in Lemma 4.1 shows that the angles $\theta_{\pm k}$ where $k = 2 \sim n + 1$ are the $2n$ roots of the following equation in the interval $(0, \pi)$.

$$\frac{\sin(n+1)\theta}{\sin n\theta} = \mp \frac{1}{\sqrt{2}}. \quad (59)$$

Remark 4.3. Equation (59) is almost the same as the one presented in Ref. [17], but the RHS there is $\pm\sqrt{2}$. Therefore our analysis shown below is slightly different from those shown in Ref. [26] (which contains a review and some improvements of the results in Ref. [17]).

For an intuitive understanding of Eq. (59), its LHS for $n = 8$ and the horizontal lines $y = 0, \pm \frac{1}{\sqrt{2}}$ are plotted in Fig. 5.

We now present Lemma 4.4 showing that $\Delta_\theta = \Omega(1/n)$ with our choice of S' .

Lemma 4.4. When n is sufficiently large, the minimal gap Δ_θ of the roots of Eq. (59) has the following $\Omega(1/n)$ lower bound with $S' = (\frac{\pi}{3}, \frac{2\pi}{3})$:

$$\Delta_\theta = \min\{|\theta_{\pm k} - \theta_{\pm j}| : \theta_{\pm k} \in S', \theta_{\pm j} \in (0, \pi), k \neq j\} \quad (60)$$

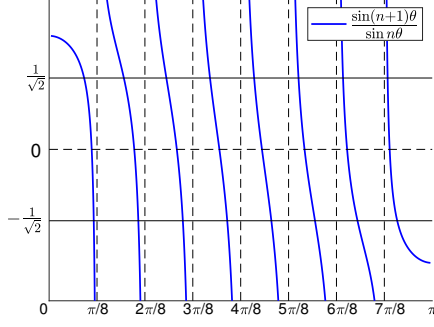


Fig. 5 Left hand side of Eq. (59) for $n = 8$.

$$\geq \frac{\pi - 2\theta_0}{n} \approx \frac{0.15\pi}{n}, \quad (61)$$

where $\tan \theta_0 = \frac{\sqrt{3}}{\sqrt{2}-1}$.

Proof. By centrosymmetry, we only need to consider the angle gap between the root $\theta = \frac{l\pi}{n} - \delta$ corresponding to RHS = $-\frac{1}{\sqrt{2}}$ in Eq. (59) and the root $\theta' = \frac{l'\pi}{n} + \delta'$ corresponding to RHS = $\frac{1}{\sqrt{2}}$ in Eq. (59), where $l' \in \{l-1, l\}$. Since the $(n-1)$ zeros $\frac{l\pi}{n}$ of $\sin n\theta$ correspond to the vertical asymptotes of LHS of Eq. (59), we have $\delta, \delta' \in (0, \frac{\pi}{n})$.

We now consider the lower and upper bound of δ . Substituting $\theta = \frac{l\pi}{n} - \delta$ into Eq. (59), and using the trigonometric identity $\sin(a-b) = \sin(a)\cos(b) - \cos(a)\sin(b)$, we have

$$-\sqrt{2} \sin(n\theta + \theta) = \sin(n\theta) \quad (62)$$

$$\Leftrightarrow -\sqrt{2} \sin(l\pi - n\delta + \frac{l\pi}{n} - \delta) = \sin(l\pi - n\delta) \quad (63)$$

$$\Leftrightarrow -\sqrt{2} \sin(n\delta - \frac{l\pi}{n} + \delta) = \sin(n\delta) \quad (64)$$

$$\Leftrightarrow -\sqrt{2} \sin(n\delta - \theta) = \sin(n\delta) \quad (65)$$

$$\Leftrightarrow -\sqrt{2} [\sin(n\delta) \cos \theta - \cos(n\delta) \sin \theta] = \sin(n\delta) \quad (66)$$

$$\Leftrightarrow -\sqrt{2} [\tan(n\delta) \cos \theta - \sin \theta] = \tan(n\delta) \quad (67)$$

Thus

$$\tan(n\delta) = \frac{\sqrt{2} \sin \theta}{1 + \sqrt{2} \cos \theta}. \quad (68)$$

Since the RHS of Eq. (68) is monotone increasing on $(\frac{\pi}{3}, \frac{2\pi}{3}) \ni \theta$, we have $\frac{\sqrt{3}}{\sqrt{2}+1} < \tan(n\delta) < \frac{\sqrt{3}}{\sqrt{2}-1}$, from which $\frac{\theta_1}{n} < \delta < \frac{\theta_0}{n}$, where $\theta_1 = \arctan \frac{\sqrt{3}}{\sqrt{2}+1}$.

We now consider the lower and upper bound of δ' . If we Substitute $\theta' = \frac{l'}{n}\pi + \delta'$ into Eq. (59), we have

$$\tan(n\delta') = \frac{\sqrt{2} \sin \theta'}{1 - \sqrt{2} \cos \theta'}. \quad (69)$$

Similarly, it can be shown that $\frac{\theta_1}{n} < \delta' < \frac{\theta_0}{n}$. Therefore, $\Delta_\theta \geq \min\{\frac{\pi}{n} - 2\frac{\theta_0}{n}, 2\frac{\theta_1}{n}\} = \frac{\pi - 2\theta_0}{n} \approx \frac{0.15\pi}{n}$. \square

4.4 Proof of Theorem 4.1

With the help of the above three Lemmas 4.1-4.4, We can now prove Theorem 4.1.

In order to lower bound the items $|y_j^* c_j|$ of the sum in Eq. (38) in Lemma 4.2, we first calculate:

$$\langle 2n+1, L | u_{\pm, \pm k} \rangle \langle u_{\pm, \pm k} | 0, R \rangle \quad (70)$$

$$= \langle 2n+1, L | \cdot (|a_{\pm k}\rangle - \exp(\pm i\varphi_{\pm k}) |b_{\pm k}\rangle) \cdot (\langle a_{\pm k}| - \exp(\pm i\varphi_{\pm k}) \langle b_{\pm k}|) \cdot |0, R\rangle \quad (71)$$

$$= [v_{\pm k}(1) - e^{\pm i\varphi_{\pm k}} \sqrt{p} v_{\pm k}(2)] \cdot [v_{\pm k}(1) - e^{\mp i\varphi_{\pm k}} \sqrt{p} v_{\pm k}(2)] \cdot (\pm_k) \quad (72)$$

$$= [v_{\pm k}(1)^2 + p v_{\pm k}(2)^2 - 2\lambda_{\pm k} v_{\pm k}(1) v_{\pm k}(2)] \cdot (\pm_k) \quad (73)$$

$$= (\pm_k)(1 - \lambda_k^2). \quad (74)$$

The last line follows from $v_{\pm k}(1) = 1$ and $v_{\pm k}(2) = \lambda_{\pm k}/\sqrt{p}$. Therefore, combined with the norm $\| |u_k\rangle \|$ shown by Eq. (35) in Lemma 4.1, we have the following identities when $\theta_k \in S'$.

$$| \langle 2n+1, L | \Pi_{|u_{\pm, \pm k}\rangle} | 0, R \rangle | = \frac{1 - \lambda_k^2}{\| |u_k\rangle \|^2} \quad (75)$$

$$= \frac{q}{2} \cdot \frac{\sin^2 \theta_k}{1 - \lambda_k^2} \left(n + \sqrt{\frac{q}{p}} \frac{\sin((n+1)2\theta_k)}{2 \sin \theta_k} \right)^{-1} \quad (76)$$

$$\geq \frac{1}{3} \cdot \frac{3}{4} \cdot \left(n + \sqrt{2} \frac{1}{2 \cdot \sqrt{3}/2} \right)^{-1} \quad (77)$$

$$\geq \frac{1}{4n} + O\left(\frac{1}{n^2}\right). \quad (78)$$

The third line above follows from $\theta_k \in (\frac{\pi}{3}, \frac{2\pi}{3})$. Since θ_k is almost uniformly distributed in $(0, \pi)$, we have $\sum_{j \in S} |y_j^* c_j|^2 \geq \frac{1}{3} \cdot 4n \cdot \left(\frac{1}{4n}\right)^2 = \frac{1}{12n}$.

We set

$$k \geq \log 24n, \quad (79)$$

and

$$T \geq \frac{\pi}{2\Delta E_S}, \quad (80)$$

which is approximately $\frac{n}{0.3\sqrt{6/7}} \approx 3.6n$ by Lemma 4.4 and Eq. (58). Then $\left(\frac{\pi}{T\Delta E_S}\right)^k \leq \left(\frac{1}{2}\right)^{\log 24n} = \frac{1}{24n}$. And thus by Eq. (38),

$$p(y|\psi_0) \geq \sum_{j \in S} |y_j^* c_j|^2 - \left(\frac{\pi}{T\Delta E_S}\right)^k \quad (81)$$

$$\geq \frac{1}{12n} - \frac{1}{24n} = \frac{1}{24n}. \quad (82)$$

Note that $p(t) = |\langle 4n+1 | M_U^t | 0 \rangle|^2 = 0$ when $t < 2n$. In fact, $M_U |0\rangle = |1\rangle$ and one iteration of M_U can propagate the amplitude from $|k\rangle$ to at furthest $|k+2\rangle$, thus $p(t) = 0$ when $t < 2n$. Since maximum is greater than average, we have now proven Theorem 4.1.

Remark 4.4. We can actually obtain an explicit expression of $A(t) := \langle 4n+1 | M_U^t | 0 \rangle$ for odd t as

$$A(t) = \frac{p-q}{2p-(q/p)^n} + 2q \sum_{k=2}^{n+1} \frac{\cos(t \arccos(2\sqrt{pq} \cos \theta_k))}{1-4pq \cos^2 \theta_k} \frac{\sin^2 \theta_k}{n + \sqrt{\frac{q}{p}} \frac{\sin((n+1)2\theta_k)}{2 \sin \theta_k}}. \quad (83)$$

Since the expression is too complicated, our first attempt of directly analyzing $A(t)$ fails, and thus we have turned to the help of Lemma 4.2.

$A(t)$ can be calculated as follows. By Eq. (74) and the expression of $|u_{\pm 1}\rangle$ shown in Lemma 4.1, we have

$$A(t) = \sum_{\pm} \sum_{\pm_k} \sum_{k=2}^{n+1} e^{\pm it \varphi_{\pm k}} \frac{(\pm_k)(1-\lambda_k^2)}{\| |u_k\rangle \|^2} + \sum_{\pm} (\pm)^t \frac{(\pm)}{\| |u_1\rangle \|^2}. \quad (84)$$

Note that

$$\sum_{\pm} e^{\pm it \varphi_{\pm k}} = 2 \cos(t \varphi_{\pm k}). \quad (85)$$

Since $\varphi_{-k} = \pi - \varphi_k$, we have

$$\sum_{\pm_k} \cos(t \varphi_{\pm k})(\pm_k) = \cos(t \varphi_k)(1 - (-1)^t). \quad (86)$$

Similarly,

$$\sum_{\pm} (\pm)^t (\pm) = 1 - (-1)^t. \quad (87)$$

Therefore, it can be seen that

$$A(t) = 0, \quad \text{if } t \text{ is even.} \quad (88)$$

Thus we will only consider odd t . Substituting the square of norms $\| |u_{\pm k}\rangle \|^2, k = 1 \sim (n+1)$ in Lemma 4.1, we have $A(t)$ as shown in Eq. (83).

5 Deterministic quantum algorithm with $O(n^{1.5} \log n)$ queries

With the matrix expression $M_U = M_S \cdot M_C$ of U_{walk} within its reduced invariant subspace \mathcal{H}_0 obtained in Section 3, the exact value of the amplitude on the target state after $T_1 = O(n \log n)$ steps of quantum walks, i.e. $\langle 4n+1 | M_U^{T_1} | 0 \rangle$, can be calculated exactly. Therefore, combining with one of the deterministic quantum search algorithms [33], for example Long's algorithm [34], we can design a deterministic quantum algorithm for the welded tree problem as shown in Algorithm 2.

More precisely, if there is a quantum process (unitary operation) \mathcal{A} that transform some initial state $|0\rangle$ to $|\psi\rangle$ that has known overlap, i.e. $p = |\langle t | \psi \rangle| \in (0, 1)$, with the desired target state $|t\rangle$. Then Long's algorithm [34] can amplify the overlap to 1 by applying the generalized Grover's iteration $G(\alpha, \beta) = \mathcal{A}S_0(\beta)\mathcal{A}^\dagger \cdot S_t(\alpha)$, where $S_t(\alpha) = e^{i\alpha|t\rangle\langle t|}$ and $S_0(\beta) = e^{-i\beta|0\rangle\langle 0|}$, for $T = O(1/p)$ times to the state $|\psi\rangle = \mathcal{A}|0\rangle$.

In the case of the original Grover's algorithm [35], $\mathcal{A} := H^{\otimes n}$ is the Hadarmard gates on n qubits, $|0\rangle := |0\rangle^{\otimes n}$, and $|t\rangle$ is the equal-superposition of all target elements. In the case of Algorithm 2, $\mathcal{A} := U_{\text{walk}}^{T_1} U_p$, $|0\rangle := |s, \perp\rangle$, and $|t\rangle := |t, \varphi(t)\rangle$. The parameters T, α, β are determined by the known overlap p , where in Grover's case is the square root of the proportion of target elements in the unstructured database, and in our case is $p_{T_1} = |\langle 4n+1 | M_U^{T_1} | 0 \rangle| = \Omega(1/\sqrt{n})$.

Algorithm 2 Deterministic quantum algorithm for the welded tree problem

Input: adjacency list quantum oracle O (see Eq. (2)) for the welded tree G_n , and the entrance name $s \equiv 0^{2n}$.

Output: the exit name t .

Procedure:

1. Same as step 1 in Algorithm 1.
 2. Construct quantum circuit of the generalized Grover's iteration $G(\alpha, \beta) = \mathcal{A}S_0(\beta)\mathcal{A}^\dagger \cdot S_t(\alpha)$ as in Fig. 6, where $\mathcal{A} := U_{\text{walk}}^{T_1} U_p$. Set the parameters α, β, T_2 as $\alpha = -\beta = 2 \arcsin\left(\frac{\sin \frac{\pi}{4T_2+2}}{\sin \theta}\right)$ and $T_2 = \lceil \frac{\pi/2-\theta}{2\theta} \rceil$, where $\theta = \arcsin(p_{T_1})$.
 3. Apply $G(\alpha, \beta)^{T_2}$ to $|\psi_{T_1}\rangle = \mathcal{A}|s, \perp\rangle$. This will result in $|t, \varphi(t)\rangle$ exactly and thus measuring register r_1 leads to the exit name t with certainty.
-

6 Numerical simulation suggests better query complexity

We find that the actual performance of our algorithms is better than $O(n^{1/2} \cdot n \log n)$, since results of numerical simulation (conducted by MATLAB) show that the success amplitude will be $\Omega(n^{-1/3})$ when U_{walk} is applied for $O(n)$ times. We formalize it in the following Conjecture 6.1 (an improved version of Theorem 4.1). Then the query complexity of Algorithm 2 will be $O(n^{1/3} \cdot n) = O(n^{4/3})$.

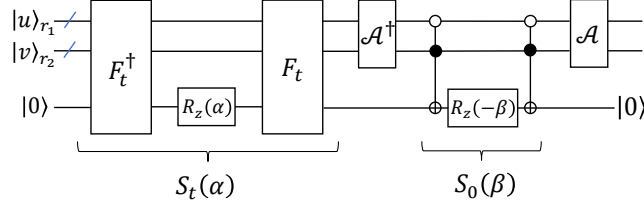


Fig. 6 Quantum circuit implementing the generalized Grover's iteration $G(\alpha, \beta) = \mathcal{A}S_0(\beta)\mathcal{A}^\dagger \cdot S_t(\alpha)$. Single qubit operation $R_z(\alpha) := \text{diag}(1, e^{i\alpha})$. Operator $S_0(\beta)$ add phase shift $e^{-i\beta}$ to the initial state $|s, \perp\rangle = |0^{2n}, 1^{2n}\rangle$, and operator F_t flip the last auxiliary qubit conditioned on $|u\rangle_{r_1} = |t\rangle$. Determining that $u = t$ can be done by querying the three adjacent vertices of u and checking that exactly one of them is \perp and $u \neq s$.

Conjecture 6.1. *There exists odd number $T \in [2n, 2.5n]$ ($T \approx n/\sqrt{pq} \approx 2.1213n$ for sufficient large n) such that*

$$|A(T)| = |\langle 4n + 1 | M_U^T | 0 \rangle| > n^{-1/3}. \quad (89)$$

Remark 6.1. *We only consider odd T because Eq. (88) shows that $p_T = 0$ when T is even. The constant \sqrt{pq} may come from the fact that $g'(\pi/2) = 2\sqrt{pq}$ (see Eq. (56)) and $2\pi/g'(\pi/2) = 1/\sqrt{pq}$.*

One can obtain the exact value of the largest $|A(t)|$ with $t \in [2n, 2.5n]$ (denoted by A_T) using, for example, MATLAB's Symbolic Math Toolbox. The exact value of A_T when $n = 50, 100, 150$ is shown in Table 2.

Table 2 The exact value of A_T when $n = 50, 100, 150$.

n	T	A_T
50	109	$2^{152} \cdot 19 \cdot 38861/3^{108}$
100	215	$2^{300} \cdot 318388779301/3^{214}$
150	323	$2^{451} \cdot 274739 \cdot 1231103390273/3^{322}$

The scatter diagram of A_T for $n = 3, \dots, 1000$ is shown in Fig. 7. It can be seen that $\log_2(A_T) > -1/3 \cdot \log_2(n)$ holds for all $n \in [6, 1000]$, which supports Conjecture 6.1.

The scatter diagram of the ratio T/n for $n = 3, \dots, 1000$ is shown in Fig. 8. It can be seen that T/n tends to $\frac{1}{\sqrt{pq}} = \frac{3}{\sqrt{2}} \approx 2.12$ as $n \rightarrow \infty$.

We also depict, as an example $n = 200$, evolution of the $(4n + 2)$ -dimensional vector $|\psi_T\rangle = M_U^T |0\rangle$ for odd T ranging from 1 to $2.5n$ in video [36]. The frame when $T = 429$ of the video is shown in Fig. 9. It can be seen that the amplitude of the state vector $|\psi_T\rangle$ can be positive or negative, showing the periodic coherent and destructive nature of quantum walk.

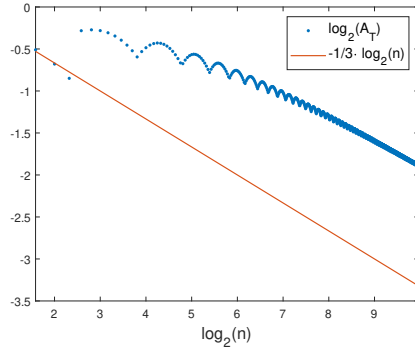


Fig. 7 Scatter diagram of $\log_2(A_T)$ for $n = 3, \dots, 1000$. Orange solid line represents $-1/3 \cdot \log_2(n)$.

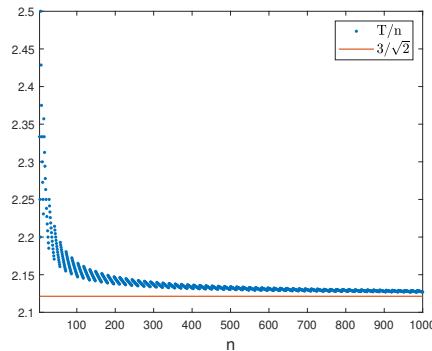


Fig. 8 Scatter diagram of T/n for $n = 3, \dots, 1000$. The horizontal line represents $\frac{1}{\sqrt{pq}} = \frac{3}{\sqrt{2}}$.

7 Conclusion

In this paper, we have revisited quantum algorithms for the welded tree problem and proposed a rather succinct algorithm based purely on the simplest coined quantum walks. A rigorous polynomial query upper bound is provided based on spectral decomposition of the reduced quantum walk matrix. The succinctness of our algorithm re-displays the power of the simplest framework of quantum walks, changing the stereotype that coined quantum walks can only achieve a quadratic speedup over classical algorithms. Our algorithm for the welded tree problem can also be made deterministic theoretically, making it one of the few examples of an exponential separation between the deterministic (exact) quantum and the randomized query complexities. Numerical simulation indicates that the actual performance of our algorithms is better, and a natural follow-up work is to rigorously prove Conjecture 6.1.

Acknowledgments. We would like to thank Yongzhen Xu and Qingwen Wang for helpful discussions on quantum walk search frameworks. We would also like to thank the reviewers of SODA2024 for suggestions which have improved the presentation of the paper. This work is supported by the National Natural Science Foundation of

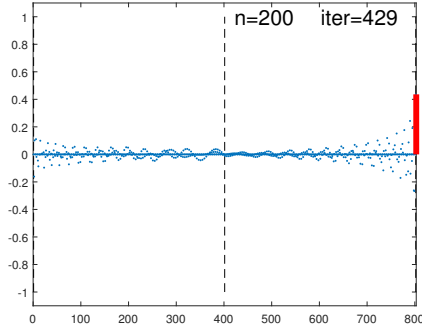


Fig. 9 The frame when $T = 429$ of the video [36] showing the evolution of the $(4n + 2)$ -dimensional vector $|\psi_T\rangle$ with $n = 200$. The x -axis represents the indices $k \in \{0, \dots, 4n + 1\}$ of $|\psi_T\rangle$, and the y -axis represents the amplitude of the k -th component, which is between $[-1, 1]$. The red pillar on the rightmost represents the amplitude $\langle 4n + 1 | \psi_T \rangle$.

China (Grant No. 62272492), and the Guangdong Basic and Applied Basic Research Foundation (Grant No. 2020B1515020050).

Declarations

Conflict of interest. The authors declare that they have no known competing financial interests or personal relationships that could have appeared to influence the work reported in this paper.

References

- [1] Aharonov, Y., Davidovich, L., Zagury, N.: Quantum random walks. *Phys. Rev. A* **48**, 1687–1690 (1993) <https://doi.org/10.1103/PhysRevA.48.1687>
- [2] Kempe, J.: Quantum random walks: An introductory overview. *Contemporary Physics* **44**(4), 307–327 (2003) <https://doi.org/10.1080/00107151031000110776>
- [3] Ambainis, A.: Quantum walks and their algorithmic applications. *International Journal of Quantum Information* **01**(04), 507–518 (2003) <https://doi.org/10.1142/S0219749903000383>
- [4] Venegas-Andraca, S.E.: Quantum walks: a comprehensive review. *Quantum Information Processing* **11**(5), 1015–1106 (2012) <https://doi.org/10.1007/s11128-012-0432-5>
- [5] Kadian, K., Garhwal, S., Kumar, A.: Quantum walk and its application domains: A systematic review. *Computer Science Review* **41**, 100419 (2021) <https://doi.org/10.1016/j.cosrev.2021.100419>

- [6] Ambainis, A., Bach, E., Nayak, A., Vishwanath, A., Watrous, J.: One-dimensional quantum walks. In: Proceedings of the 33rd ACM Symposium on Theory of Computing, pp. 37–49 (2001). <https://doi.org/10.1145/380752.380757> . <https://doi.org/10.1145/380752.380757>
- [7] Aharonov, D., Ambainis, A., Kempe, J., Vazirani, U.V.: Quantum walks on graphs. In: Proceedings of the 33rd ACM Symposium on Theory of Computing, pp. 50–59 (2001). <https://doi.org/10.1145/380752.380758> . <https://doi.org/10.1145/380752.380758>
- [8] Szegedy, M.: Quantum speed-up of markov chain based algorithms. In: 45th Annual IEEE Symposium on Foundations of Computer Science, pp. 32–41 (2004). <https://doi.org/10.1109/FOCS.2004.53>
- [9] Magniez, F., Nayak, A., Roland, J., Santha, M.: Search via quantum walk. *SIAM J. Comput.* **40**(1), 142–164 (2011) <https://doi.org/10.1137/090745854>
- [10] Krovi, H., Magniez, F., Ozols, M., Roland, J.: Quantum walks can find a marked element on any graph. *Algorithmica* **74**(2), 851–907 (2016) <https://doi.org/10.1007/s00453-015-9979-8>
- [11] Belovs, A.: Quantum Walks and Electric Networks (2013)
- [12] Apers, S., Gilyén, A., Jeffery, S.: A Unified Framework of Quantum Walk Search. In: Bläser, M., Monmege, B. (eds.) 38th International Symposium on Theoretical Aspects of Computer Science (STACS 2021). Leibniz International Proceedings in Informatics (LIPIcs), vol. 187, pp. 6–1613. Schloss Dagstuhl – Leibniz-Zentrum für Informatik, Dagstuhl, Germany (2021). <https://doi.org/10.4230/LIPIcs.STACS.2021.6> . <https://drops.dagstuhl.de/opus/volltexte/2021/13651>
- [13] Ambainis, A.: Quantum walk algorithm for element distinctness. *SIAM J. Comput.* **37**(1), 210–239 (2007) <https://doi.org/10.1137/S0097539705447311>
- [14] Buhrman, H., Spalek, R.: Quantum verification of matrix products. In: Proceedings of the Seventeenth ACM-SIAM Symposium on Discrete Algorithms, pp. 880–889 (2006). <http://dl.acm.org/citation.cfm?id=1109557.1109654>
- [15] Magniez, F., Santha, M., Szegedy, M.: Quantum algorithms for the triangle problem. *SIAM J. Comput.* **37**(2), 413–424 (2007) <https://doi.org/10.1137/050643684>
- [16] Magniez, F., Nayak, A.: Quantum complexity of testing group commutativity. *Algorithmica* **48**(3), 221–232 (2007) <https://doi.org/10.1007/s00453-007-0057-8>
- [17] Childs, A.M., Cleve, R., Deotto, E., Farhi, E., Gutmann, S., Spielman, D.A.: Exponential algorithmic speedup by a quantum walk. In: Proceedings of the Thirty-Fifth Annual ACM Symposium on Theory of Computing. STOC '03,

- pp. 59–68. Association for Computing Machinery, New York, NY, USA (2003). <https://doi.org/10.1145/780542.780552> . <https://doi.org/10.1145/780542.780552>
- [18] Childs, A.M., Farhi, E., Gutmann, S.: An example of the difference between quantum and classical random walks. *Quantum Information Processing* **1**(1), 35–43 (2002) <https://doi.org/10.1023/A:1019609420309>
- [19] Kempe, J.: Quantum Random Walks Hit Exponentially Faster (2002)
- [20] Jeffery, S., Zur, S.: Multidimensional quantum walks. In: Proceedings of the 55th Annual ACM Symposium on Theory of Computing, STOC 2023, pp. 1125–1130. Association for Computing Machinery, New York, NY, USA (2023). <https://doi.org/10.1145/3564246.3585158> . <https://doi.org/10.1145/3564246.3585158>
- [21] Childs, A.M., Wang, D.: Can graph properties have exponential quantum speedup? (2020)
- [22] Ben-David, S., Childs, A.M., Gilyén, A., Kretschmer, W., Podder, S., Wang, D.: Symmetries, graph properties, and quantum speedups. In: 2020 IEEE 61st Annual Symposium on Foundations of Computer Science (FOCS), pp. 649–660 (2020). <https://doi.org/10.1109/FOCS46700.2020.00066>
- [23] Brassard, G., Hoyer, P.: An exact quantum polynomial-time algorithm for simon’s problem. In: Proceedings of the Fifth Israeli Symposium on Theory of Computing and Systems, pp. 12–23 (1997). <https://doi.org/10.1109/ISTCS.1997.595153>
- [24] Ye, Z., Huang, Y., Li, L., Wang, Y.: Query complexity of generalized simon’s problem. *Information and Computation* **281**, 104790 (2021) <https://doi.org/10.1016/j.ic.2021.104790>
- [25] Ide, Y., Konno, N., Segawa, E., Xu, X.-P.: Localization of discrete time quantum walks on the glued trees. *Entropy* **16**(3), 1501–1514 (2014) <https://doi.org/10.3390/e16031501>
- [26] Atia, Y., Chakraborty, S.: Improved upper bounds for the hitting times of quantum walks. *Phys. Rev. A* **104**, 032215 (2021) <https://doi.org/10.1103/PhysRevA.104.032215>
- [27] Gilyén, A., Su, Y., Low, G.H., Wiebe, N.: Quantum singular value transformation and beyond: Exponential improvements for quantum matrix arithmetics. In: Proceedings of the 51st Annual ACM SIGACT Symposium on Theory of Computing, STOC 2019, pp. 193–204. Association for Computing Machinery, New York, NY, USA (2019). <https://doi.org/10.1145/3313276.3316366> . <https://doi.org/10.1145/3313276.3316366>
- [28] Yoder, T.J., Low, G.H., Chuang, I.L.: Fixed-point quantum search with an optimal number of queries. *Phys. Rev. Lett.* **113**, 210501 (2014) <https://doi.org/10.1103/PhysRevLett.113.210501>

- [29] Fenner, S.A., Zhang, Y.: A note on the classical lower bound for a quantum walk algorithm (2003)
- [30] Childs, A.M.: On the relationship between continuous- and discrete-time quantum walk. *Communications in Mathematical Physics* **294**(2), 581–603 (2010) <https://doi.org/10.1007/s00220-009-0930-1>
- [31] Kitaev, A.Y.: Quantum measurements and the Abelian Stabilizer Problem. arXiv (1995). <https://doi.org/10.48550/ARXIV.QUANT-PH/9511026> . <https://arxiv.org/abs/quant-ph/9511026>
- [32] Bernstein, E., Vazirani, U.: Quantum complexity theory. In: Proceedings of the Twenty-Fifth Annual ACM Symposium on Theory of Computing. STOC '93, pp. 11–20. Association for Computing Machinery, New York, NY, USA (1993). <https://doi.org/10.1145/167088.167097> . <https://doi.org/10.1145/167088.167097>
- [33] Li, G., Li, L.: Deterministic quantum search with adjustable parameters: Implementations and applications. *Information and Computation* **292**, 105042 (2023) <https://doi.org/10.1016/j.ic.2023.105042>
- [34] Long, G.L.: Grover algorithm with zero theoretical failure rate. *Phys. Rev. A* **64**, 022307 (2001) <https://doi.org/10.1103/PhysRevA.64.022307>
- [35] Grover, L.K.: A fast quantum mechanical algorithm for database search. In: Proceedings of the Twenty-Eighth Annual ACM Symposium on Theory of Computing. STOC '96, pp. 212–219. Association for Computing Machinery, New York, NY, USA (1996). <https://doi.org/10.1145/237814.237866> . <https://doi.org/10.1145/237814.237866>
- [36] Evolution of the reduced state vector of DTQW on welded tree. <https://www.bilibili.com/video/BV1kK411179r/>
- [37] Jordan, C.: Essai sur la géométrie à n dimensions. *Bulletin de la Société Mathématique de France* **3**, 103–174 (1875)
- [38] Li, G., Li, L.: Optimal exact quantum algorithm for the promised element distinctness problem (2022). <https://arxiv.org/abs/2211.05443>

Appendix A Implementing U_φ in Lemma 2.1

In this appendix, we will implement the unitary operator $U_\varphi : |u, \perp\rangle \mapsto |u, \varphi(u)\rangle$ in Lemma 2.1. We first introduce five auxiliary registers

$$|0\rangle_{q_1} |0\rangle_{q_2} |0\rangle_{q_3} |0\rangle_a |0\rangle_b |0\rangle_c, \quad (\text{A1})$$

where register q_i consists of $2n$ qubits storing the query result, register a is a qutrit with state space $\mathbb{H}^3 = \text{span}\{|0\rangle, |1\rangle, |2\rangle\}$ used for generating $|\varphi(u)\rangle$ when u is an internal node, register b is a qudit with state space $\mathbb{H}^5 = \text{span}\{|0\rangle, \dots, |4\rangle\}$ storing conditions, and register c is a qubit used for generating $|\varphi(u)\rangle$ when u is one of the roots. Now U_φ can be implemented as follows, where oracle query happens in the first and last step.

1. Query the oracle O on registers r_1, q_1, q_2, q_3 to obtain

$$|u\rangle_{r_1} |\perp\rangle_{r_2} \bigotimes_{i=1}^3 |\Gamma(u, i)\rangle_{q_i} |0\rangle_a |0\rangle_b |0\rangle_c. \quad (\text{A2})$$

2. Apply the transformation $|q\rangle |b\rangle \mapsto |q\rangle |b + f(q)\rangle$ on register $q := (q_1, q_2, q_3)$ and b . The function $f : \{0, 1\}^{6n} \rightarrow \{0, \dots, 4\}$ is defined as: $f(q) = 0$ iff there's no $q_i = \perp$, so that u is an internal node; $f(q) = i$ for $i = 1, 2, 3$ iff there's one and only one $q_i = \perp$, so that $u \in \{s, t\}$, and the i th register q_i stores the value \perp ; $f(q) = 4$ iff there's more than one $q_i = \perp$, so that $u \notin V(G_n)$. *It can be easily seen that calculating f takes $O(n)$ basic operations.*

3. Conditioned on $b = 0$, i.e. u is an internal node, apply the following two steps.

- 3.1. Flip all the qubits of register r_2 so that it's set to $|0^{2n}\rangle$. Apply quantum Fourier transform QFT_3 to register a , and then controlled by $|i\rangle_a$, $i \in \{0, 1, 2\}$, add (i.e. bit-wise modulo 2 addition) the value of register $q_{(i+1)}$ to register r_2 , obtaining

$$|u\rangle_{r_1} \left(\frac{1}{\sqrt{3}} \sum_{i=0}^2 |\Gamma(u, i+1)\rangle_{r_2} |i\rangle_a \right) \bigotimes_{i=0}^2 |\Gamma(u, i+1)\rangle_{q_{(i+1)}} |b\rangle_b |0\rangle_c. \quad (\text{A3})$$

This controlled addition can be done in $O(n)$ basic operations.

- 3.2. Compare $|\Gamma(u, i)\rangle_{r_2}$ with $|\Gamma(u, j)\rangle_{q_j}$ for $j = 1, 2, 3$ and subtract $|i\rangle_a$ with $(j-1)$, where j is the *unique* index j such that $|\Gamma(u, i)\rangle_{r_2} = |\Gamma(u, j)\rangle_{q_j}$, obtaining

$$|u\rangle_{r_1} |\varphi(u)\rangle_{r_2} \bigotimes_{i=1}^3 |\Gamma(u, i)\rangle_{q_i} |0\rangle_a |b\rangle_b |0\rangle_c. \quad (\text{A4})$$

The uniqueness of the index j can be easily seen from the condition that all of u 's neighbours $\Gamma(u, i)$ are distinct. *This compare (between binary strings) and subtract operation can be done in $O(n)$ basic operations.*

4. Conditioned on $b \in \{1, 2, 3\}$, i.e. u is one of the two roots and register q_b stores \perp , apply the following steps.

- 4.1. Swap register q_b and q_3 so that the first two auxiliary registers store the genuine adjacent vertex name of $u \in \{s, t\}$. *The conditioned SWAP operation can be done in $O(n)$ basic operations.*

- 4.2. similar to step 3.1 and 3.2, transform $|\perp\rangle_{r_2}$ to $|\varphi(u)\rangle_{r_2}$ with the help of $H|0\rangle_c = \frac{1}{\sqrt{2}}(|0\rangle + |1\rangle)$.

- 4.3. Repeat step 4.1 so that the order of register q_i is restored, ensuring the success of step 7.
5. Conditioned on $b = 4$, apply the identity transformation I , since register r_1 already stores $\varphi(u) = \perp$ (the three ‘neighbours’ of $u \notin V(G_n)$ are all \perp).
6. Similar to step 2, apply the transformation $|q\rangle |b\rangle \mapsto |q\rangle |b - f(q)\rangle$ to register q, b , where the subtraction is modulo 5. Therefore, register b is recovered to $|0\rangle_b$.
7. Query the oracle O once more as in step 2, so that all the auxiliary registers are restored back to zero.

Thus U_φ can be implemented with 2 oracle queries and $O(n)$ basic operations.

Appendix B Spectral decomposition of the reduced matrix

In this Appendix, we prove Lemma 4.1 about the spectral decomposition of the reduced coined quantum walk matrix $M_U = M_S M_C$. The proof is inspired by [25]. However, since its analysis is not perfect (as they did not obtain analytical expression of U_k shown in Eq. (B42) by comparing with Chebyshev polynomial of the second kind), we will show in detail the complete proof for the sake of completeness and convenience of the readers.

We also expand or improve some of the implicit or complicated steps in [25], and point out a connection with another commonly used technique for analyzing quantum walk operators, i.e. the singular value decomposition, or more precisely, Jordan’s Lemma [37] about common invariant subspaces of two reflection operator, which has been used in Refs. [8, 10, 27, 38].

We first present the following helper Lemma B.1, which is implicit in [25] and similar to [30, Theorem 1], saying that in order to obtain the spectral decomposition of $M_U = M_S M_C$, we can instead consider the spectral decomposition of the following matrix

$$A^\dagger M_S A =: J_{2n}. \quad (\text{B5})$$

Lemma B.1. *Consider the quantum walk operator $U = \text{Ref}_B \text{Ref}_A$, where $\text{Ref}_A = (2AA^\dagger - I)$ and A is a matrix with full column rank satisfying $A^\dagger A = I$. Let*

$$|a\rangle := A|v\rangle, \quad |b\rangle := \text{Ref}_B|a\rangle, \quad (\text{B6})$$

where $\| |v\rangle \|^2 = 1$. If

$$A^\dagger \text{Ref}_B A |v\rangle = \lambda |v\rangle. \quad (\text{B7})$$

Then, when $|\lambda| < 1$, we have

$$U|u\rangle := U(|a\rangle - e^{\pm i\varphi}|b\rangle) = e^{\pm i\varphi}|u\rangle, \quad (\text{B8})$$

where $\varphi := \arccos \lambda$, and $\| |u\rangle \|^2 = 2(1 - \lambda^2)$. And when $\lambda = \pm 1$, we have

$$U|a\rangle = \pm |a\rangle. \quad (\text{B9})$$

Proof. We first consider the case when $|\lambda| < 1$. From Eq. (B7) we know

$$U|b\rangle = \text{Ref}_B(2AA^\dagger - I)(\text{Ref}_B A|v\rangle) \quad (\text{B10})$$

$$= 2\text{Ref}_B A\lambda|v\rangle - A|v\rangle \quad (\text{B11})$$

$$= 2\lambda|b\rangle - |a\rangle. \quad (\text{B12})$$

Therefore, $\text{span}\{|a\rangle, |b\rangle\}$ is an invariant subspace of U , and U takes the following matrix form:

$$L = \begin{bmatrix} 0 & -1 \\ 1 & 2\lambda \end{bmatrix}. \quad (\text{B13})$$

Let $\lambda = \cos\varphi$, then we obtain the eigenvalues and eigenvectors of L : $e^{\pm i\varphi}$ and $[1, -e^{\pm i\varphi}]^T$. This can be easily verified by the following identities:

$$1 - 2\lambda e^{\pm i\varphi} = 1 - 2\cos(\pm\varphi)e^{\pm i\varphi} \quad (\text{B14})$$

$$= 1 - 2\cos^2(\pm\varphi) - 2i\cos(\pm\varphi)\sin(\pm\varphi) \quad (\text{B15})$$

$$= -\cos(\pm 2\varphi) - i\sin(\pm 2\varphi) \quad (\text{B16})$$

$$= -e^{\pm 2i\varphi} = e^{\pm i\varphi} \cdot (-e^{\pm i\varphi}). \quad (\text{B17})$$

Therefore, we obtain two eigenvalues $e^{\pm i\varphi}$ of U and their respective eigenvectors $|u\rangle := |a\rangle - e^{\pm i\varphi}|b\rangle$. We now calculate the square of its norm:

$$\langle u|u\rangle = 2 - 2\text{Re}(e^{\pm i\varphi}\langle a|b\rangle) \quad (\text{B18})$$

$$= 2(1 - \lambda^2). \quad (\text{B19})$$

The second line follows from $\langle a|b\rangle = \langle v|A^\dagger\text{Ref}_B A|v\rangle = \lambda$ and the fact that $A^\dagger\text{Ref}_B A$ is Hermitian whose eigenvalue λ is a real number.

We now consider the case when $\lambda = \pm 1$. From Eq. (B7), we know $\langle v|A^\dagger\text{Ref}_B A|v\rangle = \pm 1$, and thus $\text{Ref}_B A|v\rangle = \pm A|v\rangle$. Therefore,

$$U|a\rangle = UA|v\rangle \quad (\text{B20})$$

$$= \text{Ref}_B(2AA^\dagger - I)A|v\rangle \quad (\text{B21})$$

$$= \text{Ref}_B A|v\rangle \quad (\text{B22})$$

$$= \pm A|v\rangle \quad (\text{B23})$$

$$= \pm |a\rangle. \quad (\text{B24})$$

□

Remark B.1. Suppose $\text{Ref}_B = 2BB^\dagger - I$. Let $D := A^\dagger B$, and consider its singular value decomposition $\sum_i s_i |v_i\rangle\langle w_i|$, which is a common approach in Refs. [8, 10, 27, 38]. Then the connection between the eigenvalue λ of $A^\dagger\text{Ref}_B A$ and the singular value s of D is:

$$\arccos(\lambda) = 2\arccos(s). \quad (\text{B25})$$

Proof. Since $DD^\dagger |v_i\rangle = s_i^2 |v_i\rangle$, we have

$$A^\dagger \text{Ref}_B A = A^\dagger (2BB^\dagger - I)A \quad (\text{B26})$$

$$= 2(A^\dagger B)(A^\dagger B)^\dagger - I \quad (\text{B27})$$

$$= 2DD^\dagger - I. \quad (\text{B28})$$

Therefore,

$$A^\dagger \text{Ref}_B A |v\rangle = \lambda |v\rangle \Leftrightarrow DD^\dagger |v\rangle = \frac{\lambda+1}{2} |v\rangle. \quad (\text{B29})$$

From the identity $\frac{\cos \phi_i + 1}{2} = \cos^2 \frac{\phi_i}{2}$, we obtain Eq.(B25). \square

We now analyze the eigenvalues and eigenvectors of $J_{2n} = A^\dagger M_S A$. First, we will need the matrix expression of J_{2n} . Recalling A as defined in Eq. (27), and since M_S swaps two adjacent rows (columns), we have:

$$A^\dagger M_S = \left[\begin{array}{cccc|c} 0 & 1 & & & \\ \sqrt{p} & 0 & 0 & \sqrt{q} & \\ & \sqrt{p} & 0 & 0 & \sqrt{q} \\ & & & \ddots & \\ & & & \sqrt{p} & 0 & 0 & \sqrt{q} \\ \hline & & & & \sqrt{q} & * & \end{array} \right]_{2(n+1) \times 2(2n+1)}. \quad (\text{B30})$$

Thus J_{2n} is a special tridiagonal and centrosymmetric matrix as shown below:

$$J_{2n} = \left[\begin{array}{cccc|c} 0 & \sqrt{p} & & & \\ \sqrt{p} & 0 & \sqrt{pq} & & \\ & \sqrt{pq} & 0 & \ddots & \\ & & \ddots & \ddots & \sqrt{pq} \\ \hline & & & \sqrt{pq} & 0 & q \\ & & & & q & * \end{array} \right]_{2(n+1) \times 2(n+1)}. \quad (\text{B31})$$

I. eigenvalues of J_{2n}

In order to calculate the characteristic equation $p(\lambda) := |\lambda I - J_{2n}|$ of J_{2n} , first introduce the following two principal submatrices. We use the notation $J_{2n}[l : k]$ to represent the main sub-matrix from l to k rows (columns) of J_{2n} , so as to save space.

$$E_k := \lambda I - J_{2n}[1 : k], \quad (\text{B32})$$

$$F_k := \lambda I - J_{2n}[2 : k+1]. \quad (\text{B33})$$

Denote by $|M| := \det(M)$ the determinant of matrix M . Then we have

$$|E_2| = \lambda |E_1| - p |E_0|, \quad (\text{B34})$$

$$|E_k| = \lambda |E_{k-1}| - pq |E_{k-2}|, \quad (3 \leq k \leq n+1) \quad (\text{B35})$$

$$|E_k| = \lambda|F_{k-1}| - p|F_{k-2}|, \quad (2 \leq k \leq n+1) \quad (\text{B36})$$

$$|F_k| = \lambda|F_{k-1}| - pq|F_{k-2}|, \quad (2 \leq k \leq n) \quad (\text{B37})$$

where the first two terms are $|F_1| = \lambda$, $|F_0| := 1$ and $|E_1| = \lambda$, $|E_0| := 1$. Note that Eq. (B35) is obtained by expanding $|E_k|$ from its lower right corner, while Eq. (B36) is obtained by expanding $|E_k|$ from its upper left corner. Eq. (B37) can be obtained by expanding $|F_k|$ from either from its upper left corner or its lower right corner. Dividing all the elements in F_k by \sqrt{pq} and denoting

$$|F_k|/\sqrt{pq}^k := U_k(\lambda/\sqrt{pq}), \quad (\text{B38})$$

Eq. (B37) is now transformed to $U_k(\lambda/\sqrt{pq}) = \lambda/\sqrt{pq} U_{k-1}(\lambda/\sqrt{pq}) - U_{k-2}(\lambda/\sqrt{pq})$. If we let $x := \frac{\lambda}{\sqrt{pq}}$, then Eq. (B37) further simplifies to

$$U_0(x) = 1, \quad U_1(x) = x, \quad (\text{B39})$$

$$U_k(x) = x U_{k-1}(x) - U_{k-2}(x). \quad (\text{B40})$$

Comparing the above equations with the recurrence relation of *Chebyshev polynomial of the second kind*:

$$\begin{aligned} \tilde{U}_0(x) &= 1, \quad \tilde{U}_1(x) = 2x, \\ \tilde{U}_k(x) &= 2x\tilde{U}_{k-1}(x) - \tilde{U}_{k-2}(x), \quad \text{for } k \geq 2, \end{aligned} \quad (\text{B41})$$

we know $U_k(x) = \tilde{U}_k(x/2)$. From the general term formula $\tilde{U}_k(\cos \theta) = \frac{\sin(k+1)\theta}{\sin \theta}$, we let θ be such that it satisfies $\cos \theta := x/2 = \frac{\lambda}{2\sqrt{pq}}$. Therefore,

$$U_k(\lambda/\sqrt{pq}) = \tilde{U}_k(\cos \theta) = \frac{\sin(k+1)\theta}{\sin \theta}. \quad (\text{B42})$$

We now calculate $p(\lambda) = |\lambda I - J_{2n}|$ by expanding its $n+1$ row as follows (cf. Eq. (B31) for J_{2n}). Denote by $E'_k = \lambda I - J_{2n}[2n+2-k+1 : 2n+2]$ the last k rows and columns of $\lambda I - J_{2n}$. It is easy to see that $|E'_k| = |E_k|$ from the centrosymmetry of J_{2n} .

$$p(\lambda) = \sqrt{pq} \begin{vmatrix} E_{n-1} & & & \\ -\sqrt{pq} & & & \\ & -\sqrt{pq} & & \\ & & -q & E'_{n+1} \end{vmatrix} + \lambda \begin{vmatrix} E_n & & & \\ & E_{n+1} & & \\ & & & \\ & & & \end{vmatrix} + q \begin{vmatrix} E_n & -\sqrt{pq} & & \\ & -q & & \\ & & -\sqrt{pq} & \\ & & & E'_n \end{vmatrix} \quad (\text{B43})$$

$$= -pq|E_{n-1}| \cdot |E_{n+1}| + \lambda|E_n| \cdot |E_{n+1}| - q^2|E_n|^2 \quad (\text{B44})$$

$$= (\lambda^2 - q^2)|E_n|^2 - 2pq\lambda|E_n| \cdot |E_{n-1}| + (pq)^2|E_{n-1}|^2 \quad (\text{B45})$$

$$= ((\lambda - q)|E_n| - pq|E_{n-1}|)((\lambda + q)|E_n| - pq|E_{n-1}|). \quad (\text{B46})$$

Note that when choosing $-q$ as the pivot to expand the first determinant in Eq. (B43), the following sub-determinant is zero.

$$\left| \begin{array}{c|c} E_{n-1} & \\ \hline -\sqrt{pq} & \\ \hline \hline & -\sqrt{pq} E'_n \end{array} \right| = 0. \quad (\text{B47})$$

This is because the first n rows are rank deficient as there are only $n-1$ columns with non zero elements. The same reasoning applies to expanding the third determinant in Eq. (B43). The third line (Eq. (B45)) uses Eq. (B35) to further expand $|E_{n+1}|$.

We can further simplify the two components of $p(\lambda)$ in Eq. (B46) by using Eqs. (B36), (B37) to expand until $|F_{n-1}|$, $|F_{n-2}|$:

$$(\lambda \mp q)|E_n| - pq|E_{n-1}| \quad (\text{B48})$$

$$= \lambda|F_n| - p|F_{n-1}| \mp q(\lambda|F_{n-1}| - p|F_{n-2}|) \quad (\text{B49})$$

$$= \lambda(\lambda|F_{n-1}| - pq|F_{n-2}|) + (\mp(1-p)\lambda - p)|F_{n-1}| \pm pq|F_{n-2}| \quad (\text{B50})$$

$$= [\lambda(\lambda \mp 1) \pm p(\lambda \mp 1)] \cdot |F_{n-1}| - pq(\lambda \mp 1)|F_{n-2}| \quad (\text{B51})$$

$$= (\lambda \mp 1) (|F_n| \pm p|F_{n-1}|). \quad (\text{B52})$$

Using Eq. (B38), we now obtain the eigenvalues of J_{2n} : ± 1 and $\lambda_{\pm k} := 2\sqrt{pq} \cos \theta_{\pm k}$, where $\lambda_{\pm k}$ are the $2n$ roots of the following equation:

$$\sqrt{q} U_n(\lambda/\sqrt{pq}) \pm \sqrt{p} U_{n-1}(\lambda/\sqrt{pq}) = 0. \quad (\text{B53})$$

Combining with Eq. (B42), we obtain Eq. (31) in Lemma 4.1. It can also be seen that when θ_k corresponds to a root with ‘+’, then $\theta_{-k} := \pi - \theta_k$ corresponds to a root with ‘-’, thus $\lambda_{-k} = -\lambda_k$.

II. eigenvectors of J_{2n}

We now consider the eigenvectors of J_{2n} . Using Eqs. (B34), (B35), and “ $(\lambda_k \mp q)|E_n| - pq|E_{n-1}| = 0$ ” by Eq. (B48), it is not difficult to verify that the respective (unnormalized) eigenvector $|v_{\pm k}\rangle$ (which satisfies $(\lambda I - J_{2n})|v_{\pm k}\rangle = 0$) is

$$\left[1, \frac{|E_1|}{\sqrt{p}}, \frac{|E_2|}{\sqrt{p}\sqrt{pq}}, \dots, \frac{|E_{n-1}|}{\sqrt{p}\sqrt{pq}^{n-2}}, \frac{|E_n|}{\sqrt{p}\sqrt{pq}^{n-1}}, \pm(*) \right], \quad (\text{B54})$$

Where $(*)$ can be deduced from centrosymmetry. Combing with the relation of the sub-determinant $|E_k|$, $|F_k|$ shown in Eqs. (B36), (B37), the components and the square of the norm of the eigenvector $|v_{\pm k}\rangle$ can be calculated as follows.

1. $\lambda = \pm 1$

Since $\lambda^2 = (\pm)^2 = 1$, we have

$$|F_k| = \pm |F_{k-1}| - pq|F_{k-2}| \quad (\text{B55})$$

$$= \pm q|F_{k-1}| \pm p(\pm |F_{k-2}| - pq|F_{k-3}|) - pq|F_{k-2}| \quad (\text{B56})$$

$$= \pm q(|F_{k-1}| - p^2|F_{k-3}|) - p^2|F_{k-2}|. \quad (\text{B57})$$

Thus we know the difference between every other term, i.e. $|F_k| - p^2|F_{k-2}|$, is a power series. Therefore,

$$|E_k| = \pm|F_{k-1}| - p|F_{k-2}| \quad (\text{B58})$$

$$= \pm|F_k| - p^2|F_{k-1}| \quad (\text{B59})$$

$$= (\pm q)^{k-2}(|F_2| - p^2|F_0|) \quad (\text{B60})$$

$$= (\pm q)^{k-2}(1 - pq - p^2) \quad (\text{B61})$$

$$= (\pm)^k q^{k-1}. \quad (\text{B62})$$

The second line follows from substituting $q = 1 - p$ into the second equality of Eq. (B37). Thus the $(i + 1)$ -th component of $|v_{\pm 1}\rangle$ is

$$\langle i|v_{\pm 1}\rangle = \frac{|E_i|}{\sqrt{p}\sqrt{pq}^{i-1}} \quad (\text{B63})$$

$$= \frac{(\pm)^i q^{i-1}}{\sqrt{p}\sqrt{pq}^{i-1}} \quad (\text{B64})$$

$$= (\pm)^i (\sqrt{q/p})^i / \sqrt{q}, \quad (\text{B65})$$

which is Eq. (29) in Lemma 4.1. Hence, the square of the norm of $|v_{\pm 1}\rangle$ is:

$$\| |v_{\pm 1}\rangle \|^2 = 2\left(1 + \frac{1}{q} \sum_{i=1}^n \left(\frac{q}{p}\right)^i\right) \quad (\text{B66})$$

$$= 2\left(1 + \frac{1}{p} \frac{1 - (q/p)^n}{1 - q/p}\right) \quad (\text{B67})$$

$$= \frac{2}{q - p} ((q/p)^n - 2p), \quad (\text{B68})$$

which is Eq. (30) in Lemma 4.1.

2. $\lambda_{\pm k}$ for $k = 2 \sim (n + 1)$

The $(i + 1)$ -th component of $|v_{\pm k}\rangle$ can be calculated as follows, where we omit the subscript “ $\pm k$ ” for simplicity.

$$\langle i|v_{\lambda}\rangle = \frac{\lambda|F_{i-1}| - p|F_{i-2}|}{\sqrt{p}\sqrt{pq}^{i-1}} \quad (\text{B69})$$

$$= \frac{\lambda\sqrt{pq}^{i-1}U_{i-1}(\lambda/\sqrt{pq}) - p\sqrt{pq}^{i-2}U_{i-2}(\lambda/\sqrt{pq})}{\sqrt{p}\sqrt{pq}^{i-1}} \quad (\text{B70})$$

$$= \frac{\lambda}{\sqrt{p}}U_{i-1}(\lambda/\sqrt{pq}) - \frac{1}{\sqrt{q}}U_{i-2}(\lambda/\sqrt{pq}), \quad (\text{B71})$$

which is Eq. (33) in Lemma 4.1, and the next Eq. (34) follows from Eq. (B42).

We now consider $\| |v_\lambda\rangle \|^2$. We first calculate the square of the $(i+1)$ -th component. For simplicity we denote $U_i(\lambda/\sqrt{pq})$ by U_i in the following.

$$|\langle i|v_\lambda\rangle|^2 = \frac{\lambda^2}{p}U_{i-1}^2 - \frac{2\lambda}{\sqrt{pq}}U_{i-1}U_{i-2} + \frac{1}{q}U_{i-2}^2 \quad (\text{B72})$$

$$= \frac{\lambda^2}{p}U_{i-1}^2 + (U_i^2 - \frac{\lambda^2}{pq}U_{i-1}^2 - U_{i-2}^2) + \frac{1}{q}U_{i-2}^2 \quad (\text{B73})$$

$$= \frac{p}{q}U_{i-2}^2 - \frac{\lambda^2}{q}U_{i-1}^2 + U_i^2. \quad (\text{B74})$$

The second line is obtained by squaring both sides of the relation $U_i = \frac{\lambda}{\sqrt{pq}}U_{i-1} - U_{i-2}$ which follows from Eq. (B40). In order to make the relation true for $i \geq 1$, we set $U_{-1} := 0$. Then, using the identity $p/q - \lambda^2/q + 1 = (1 - \lambda^2)/q$, we have

$$\| |v_\lambda\rangle \|^2/2 = 1 + \sum_{i=1}^n |\langle i|v_\lambda\rangle|^2 \quad (\text{B75})$$

$$= 1 + 0 + \frac{p}{q} - \frac{\lambda^2}{q} + \frac{1 - \lambda^2}{q} \sum_{i=1}^{n-2} U_i^2 - \frac{\lambda^2}{q}U_{n-1}^2 + U_{n-1}^2 + U_n^2 \quad (\text{B76})$$

$$= \frac{1 - \lambda^2}{q} + \frac{1 - \lambda^2}{q} \sum_{i=1}^{n-2} U_i^2 + (-\frac{\lambda^2}{q} + 1 + \frac{p}{q})U_{n-1}^2 \quad (\text{B77})$$

$$= \frac{1 - \lambda^2}{q} \sum_{i=0}^{n-1} U_i^2. \quad (\text{B78})$$

The third line uses Eq. (B53) satisfied by the eigenvalue λ . From the trigonometric expression of U_i (Eq. (B42)), we have

$$\sum_{i=0}^{n-1} U_i^2 = \frac{1}{\sin^2 \theta} \sum_{i=0}^{n-1} \sin^2(i+1)\theta \quad (\text{B79})$$

$$= \frac{1}{\sin^2 \theta} \sum_{i=1}^n \frac{1 - \cos i2\theta}{2} \quad (\text{B80})$$

$$= \frac{1}{2\sin^2 \theta} (n - \frac{\sin n\theta \cdot \cos(n+1)\theta}{\sin \theta}) \quad (\text{B81})$$

$$= \frac{1}{2\sin^2 \theta} (n \pm \sqrt{\frac{q}{p}} \frac{\sin 2(n+1)\theta}{2\sin \theta}). \quad (\text{B82})$$

Hence combined with $\| |u\rangle \|^2 = 2(1 - \lambda^2)$ in Lemma B.1 and the identity $\theta_{-k} = \pi - \theta_k$, we obtain Eq. (35) in Lemma 4.1. Note that the last line above uses Eq. (31) satisfied by θ . The third line uses the identity obtained from comparing the real part of the

following identities:

$$\sum_{k=1}^n \cos kx + i \sin kx \tag{B83}$$

$$= \sum_{k=1}^n e^{ikx} = \frac{e^{ix}(e^{inx} - 1)}{e^{ix} - 1} \tag{B84}$$

$$= \frac{e^{ix} e^{\frac{inx}{2}} 2i \sin \frac{nx}{2}}{e^{\frac{ix}{2}} 2i \sin \frac{x}{2}} = \frac{\sin \frac{nx}{2}}{\sin \frac{x}{2}} e^{i \frac{(n+1)x}{2}} \tag{B85}$$

$$= \frac{\sin \frac{nx}{2}}{\sin \frac{x}{2}} \left(\cos \frac{(n+1)x}{2} + i \sin \frac{(n+1)x}{2} \right). \tag{B86}$$